NAVAL POSTGRADUATE SCHOOL
Monterey, California

AD-A274 836

THESIS

LASER DOPPLER VELOCIMETRY
IN A LOW SPEED
MULTISTAGE COMPRESSOR

by

Joseph M. Utschig

September, 1993

Thesis Advisor: Garth V. Hobson

Approved for public release;
distribution is unlimited.

94-01956

94 1 21 138

REPORT DOCUMENTATION PAGE		Form Approved OMB No. 0704

1. AGENCY USE ONLY *(Leave blank)*	2. REPORT DATE 23 SEP 93	3. REPORT TYPE AND DATES COVERED Master's Thesis

4. TITLE AND SUBTITLE : Laser Doppler Velocimetry in a Low Speed Multistage Compressor	5. FUNDING NUMBERS
6. AUTHOR: Utschig , Joseph M.	

7. PERFORMING ORGANIZATION NAME(S) AND ADDRESS(ES) Naval Postgraduate School Monterey CA 93943-5000	8. PERFORMING ORGANIZATION REPORT NUMBER

9. SPONSORING/MONITORING AGENCY NAME(S) AND ADDRESS(ES) Director, Navy Space Systems Division (N63) Naval Air Warfare Center Space and Electronic Warfare Directorate 250 Phillips Blvd Chief of Naval Operations Princeton Crossroads Washington DC 20350-2000 Trenton, NJ 08628	10. SPONSORING/MONITORING AGENCY REPORT NUMBER

11. SUPPLEMENTARY NOTES The views expressed in this thesis are those of the author and do not reflect the official policy or position of the Department of Defense or the U.S. Government.

12a. DISTRIBUTION/AVAILABILITY STATEMENT Approved for public release; distribution is unlimited.	12b. DISTRIBUTION CODE A

13.

ABSTRACT *(maximum 200 words)*

Two-dimensional Laser Doppler Velocimetry (LDV) measurements were taken in the Low Speed Multistage Compressor (LSMSC) with data indexed to the rotor position. Laser measurements were conducted at two axial positions downstream of the second rotor and one axial position downstream of the second stator. The entire rotor periphery was measured at fixed radial displacements at each location and ensemble averaged. The survey downstream of the stator attempted to quantify the unsteady flow of the stator passage. Attempts were made to quantify the absolute flow angle behind both the rotor and the stator and compare them to pneumatic data collected at the same axial and circumferential positions respectively. Absolute flow angles calculated from the laser measurements were in agreement with pneumatic probe data. In addition, the surveys were conducted in an attempt to quantify the velocity profile from the rotor passage. The laser surveys indicated distinct and repeatable patterns in both the axial and circumferential components of the rotor exit velocity. Data downstream of the stator proved inconclusive.

14. SUBJECT TERMS: Laser Doppler Velocimetry, Rotating Frame Measurements, Low Speed Multistage Compressor			15. NUMBER OF PAGES 98
			16. PRICE CODE

17. SECURITY CLASSIFICATION OF REPORT Unclassified	18. SECURITY CLASSIFICATION OF THIS PAGE Unclassified	19. SECURITY CLASSIFICATION OF ABSTRACT Unclassified	20. LIMITATION OF ABSTRACT UL

Laser Doppler Velocimetry
in a Low Speed
Multistage Compressor

by

Joseph M. Utschig
Lieutenant, United States Navy
B.A., Marquette University, 1985

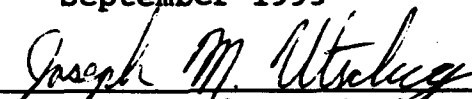Submitted in partial fulfillment
of the requirements for the degree of

MASTER OF SCIENCE IN ENGINEERING SCIENCE
(With a Major in Aeronautical Engineering)

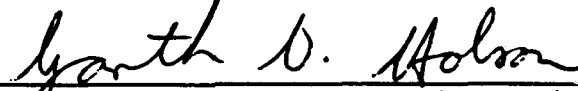from the

NAVAL POSTGRADUATE SCHOOL
September 1993

Author : _____
Joseph M. Utschig

Approved by: _____
Garth V. Hobson,   Thesis Advisor

_____
Raymond P. Shreeve, Second Reader

_____
Rudolf Panholzer, Chairman
Space Systems Academic Group

ii

ABSTRACT

Two-dimensional Laser Doppler Velocimetry (LDV) measurements were taken in the Low Speed Multistage Compressor (LSMSC) with data indexed to the rotor position. Laser measurements were conducted at two axial positions downstream of the second rotor and one axial position downstream of the second stator. The entire rotor periphery was measured at fixed radial displacements at each location and ensemble averaged. The survey downstream of the stator attempted to quantify the unsteady flow of the stator passage. Attempts were made to quantify the absolute flow angle behind both the rotor and the stator and compare them to pneumatic data collected at the same axial and circumferential positions respectively. Absolute flow angles calculated from the laser measurements were in agreement with pneumatic probe data. In addition, the surveys were conducted in an attempt to quantify the velocity profile from the rotor passage. The laser surveys indicated distinct and repeatable patterns in both the axial and circumferential components of the rotor exit velocity. Data downstream of the stator proved inconclusive.

DTIC QUALITY INSPECTED 8

Accesion For		
NTIS CRA&I	☑	
DTIC TAB	☐	
Unannounced	☐	
Justification		
By		
Distribution /		
Availability Codes		
Dist	Avail and / or Special	
A-1		

iii

TABLE OF CONTENTS

LIST OF FIGURES

LIST OF TABLES

LIST OF SYMBOLS

α	Flow angle from axial, absolute frame
β	Flow angle from axial, blade relative frame
γ	Stagger angle, from axial in the absolute frame
Δ	Incremental change in a quantity
μ	Viscosity
φ	Flow coefficient on an axisymmetric surface V_a/U
ρ	Density
σ	Blade solidity
ξ	Profile camber angle
b	Blade height or span
c	Constant or chord
D	Diffusion factor
e	Clearance gap
p	Pressure
R_u	Reynolds Number $\rho U_t c/\mu$
r	Radius of axisymmetric stream surface
T	Temperature
t	Thickness
U	Wheel velocity or peripheral velocity component measured by LDV

V	Velocity in absolute frame or axial velocity component measured by LDV
W	Velocity in relative frame

Subscripts

a	Axial direction
atmo	Atmospheric condition
R	Rotor
S	Stator
s	Static condition
t	At tip radius
u	Tangential direction
0	Stagnation condition

ACKNOWLEDGEMENTS

First and foremost I must thank Dr. Hobson for his seemingly endless patience during what turned out to be a very complicated undertaking. He always managed to smile even through the most repetitive of questions. I hope he has learned as much as I have during this time, as he has chosen to continue this line of work, while I escape back to sea.

Also among those deserving respects is Dr. Shreeve. His methodical nature and ability to laugh does set him apart from his colleagues and I have learned well from him.

Rick Still and Ted Best deserve mention as two individuals without whom my thesis would not have happened. They are two of the most capable and dedicated technicians I have come to know.

No soliloquy of mine would be complete without mentioning Dr. Boger. An administrative breath of fresh air, he never once attempted to reign me in from my rather ambitious goal, even during the darkest days of MA 1118.

And last (but certainly not least), my fiance, Martha Getris deserves a diplomatic award, for as little as she professed to understand about the subject matter, she always listened, regardless of my persistence.

I. INTRODUCTION

The flow field within a rotating axial flow compressor has several losses, or inefficiencies. Some of these include tip vortices, boundary layer separation, trailing edge vortices and wakes, and other associated flow unsteadiness. Unfortunately, most of the methods (pneumatic probes, hot-wires, etc.) that can be used to measure these phenomena are intrusive and end up contributing to the disturbance they are trying to measure. Especially in the tip clearance region of a compressor, the small area and localized flow effects are exceedingly difficult to measure and not well understood.

One of the primary non-intrusive techniques is the Laser Doppler Velocimetry (LDV) technique which was the focus of the present work. Within the last few years, several researchers have published excellent papers on LDV applications to turbomachinery.

Strazisar [Ref.1] conducted an excellent survey of LDV theory and attendant topics such as seeding, optical access to a turbomachine, and data acquisition methods. In addition, he discussed early LDV studies and their applicability.

Stauter et al. [Ref 2.] mapped the rotor and stator wake structure and decay in a large axial flow compressor. A comparison was made using the two-dimensional data to that of simultaneous pneumatic probe measurements. The experiment

1

allowed for both spatial and temporal resolution of their data. Stauter [Ref 3.] later conducted three-dimensional measurements in the tip region on the same compressor.

Chesnakas and Dancey [Ref 4.] used a system with off-axis backscatter to measure the three-dimensional flow field in the rotor blade passage of an axial compressor. This work did not, however, attempt to measure in the case wall region, stopping at only 90% of span. These were the first reported fully three-dimensional LDV measurements in a turbomachine.

Within the larger picture of the ongoing research program at the Naval Postgraduate School (NPS) Turbopropulsion ᵣ⌐aboratory (TPL), the present work was the first step towards eventually obtaining LDV measurements in both transonic turbine and compressor test rigs.

The main goal was to validate the TSI Rotating Machinery Resolver (RMR) and the Phase Resolved (PHASE) software by making measurements of flow in the Low Speed Multistage Compressor (LSMSC). This work focused on mapping the flow field directly downstream of the second rotor row and then directly downstream of the second stator row. Measurements started at approximately mid-span and proceeded outward to the casewall, with the intention of determining how close to the casewall measurements could be obtained.

The present work differs from the previous work described by Stauter in that the machine used in the present experiment had an unequal number of rotor and stator blades, while there

2

were an equal number in the experiments conducted by Stauter. Also, a much lower (by at least a factor of five) tip clearance gap was present in the LSMSC. In addition, most of the measurements in the present work concentrated in the region greater than 90% span.

II. EXPERIMENTAL APPARATUS

A. LOW SPEED MULTISTAGE COMPRESSOR

1. Overall Layout

The NPS Low Speed Multistage Compressor (LSMSC) is shown in Figure 1. The facility is an open loop, 36 inch, diameter by 35 foot long tunnel mounted horizontally in the laboratory. Ambient air is drawn from the outside and discharged into the building via a conical diffuser. The compressor the same as was reported by Moyle [Ref. 5], except that two vinyl/rubber ramp strips, intended as fairings, were removed from the inlet duct in order to decrease flow disturbances within the compressor.

Two different sizes of inlet bellmouths were available for inlet flow rate and pressure adjustment. For the present experiment, the larger bellmouth was chosen because pneumatic data as close as possible to Moyle's data [Ref. 6] were desired. Figure 2 shows the inlet bellmouth. The inlet flow was throttled by inserting discrete resistance screens into the system; there was no provision for continuous downstream throttling of the compressor while running. A complete description of the LSMSC and associated equipment is given in Reference 7.
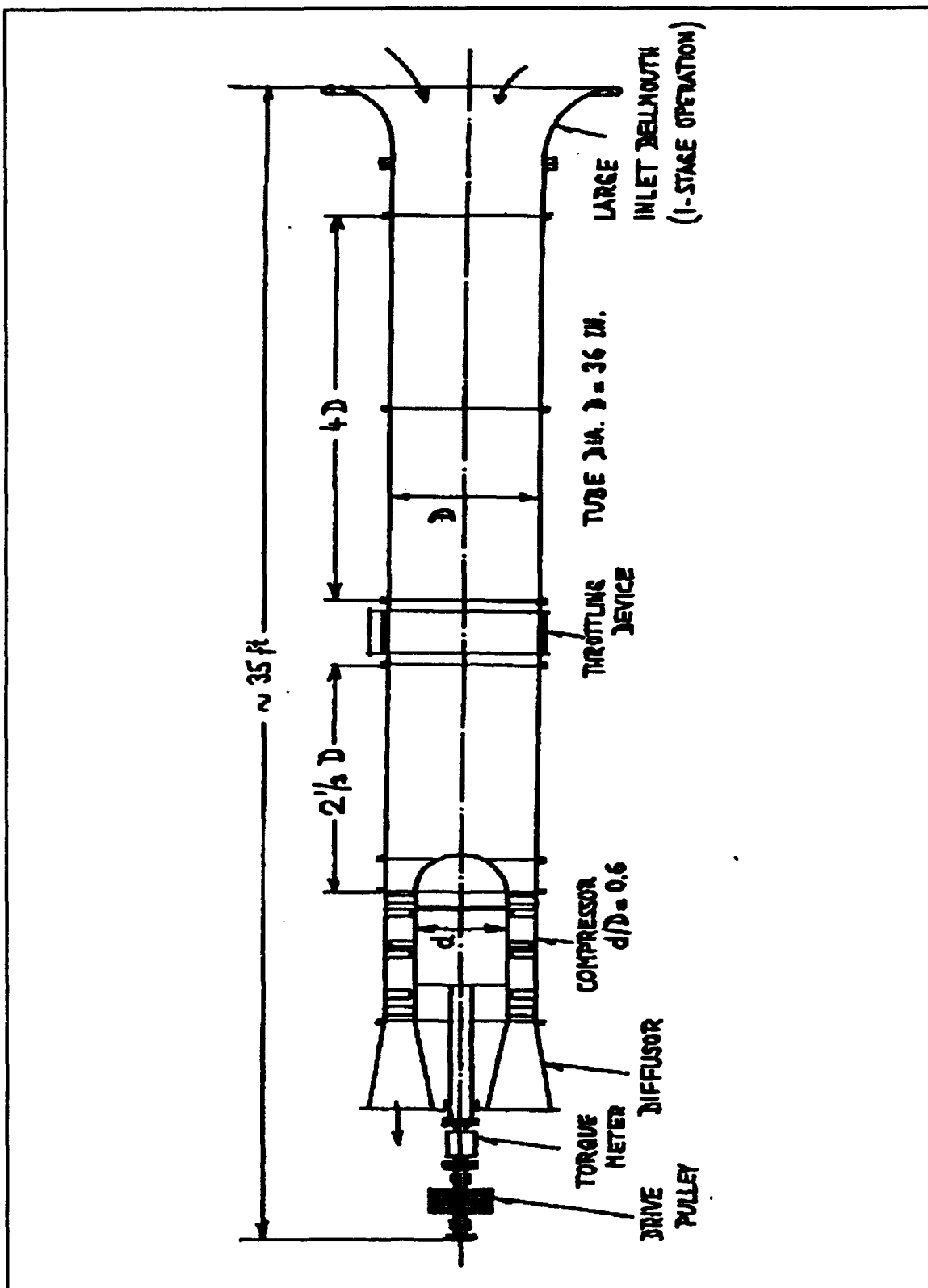
Figure 1.   Low Speed MultiStage Compressor

Figure 2.   Inlet Bellmouth With Protective Screen.

The compressor was powered by a 112 kW (150 HP) synchronous motor. Compressor rotational speed was fixed by the belt drive pulley fitted to the drive shaft. In the present study, the RPM was 1610, giving a blade tip speed of 77.8 m/s (252.9 ft/s).

2. Test Section and Blading

The compressor casing was machined from an iron casting, to leave a thick heavy wall. The fully adjustable blading consisted of an Inlet Guide Vane (IGV) row and an Exit Guide Vane (EGV) row of 30 blades each and two 30 blade rotor/32 blade stator stages.

Blade height was 7.2 inches, giving a hub-to-tip ratio of 0.6. The compressor had a design tip clearance gap (e) of 0.020 inches. The gap to blade height ratio, (e/b) was 0.004 at the second stage. The blading was of the forced-vortex type and the velocity diagrams were symmetric. The stages of the compressor were repeating stages. Figure 3 shows the velocity diagrams for one stage for both on-design and off-design conditions.

Profiles for both the rotor and stator were derived from a circular arc camber line with a modified C-4 thickness distribution. Table I [Ref. 6] gives the blading geometry. The blading was designed for a R_u of 4.2×10^5 at the tip of the blades. A complete description of the compressor blading can be found in Reference 8.

7
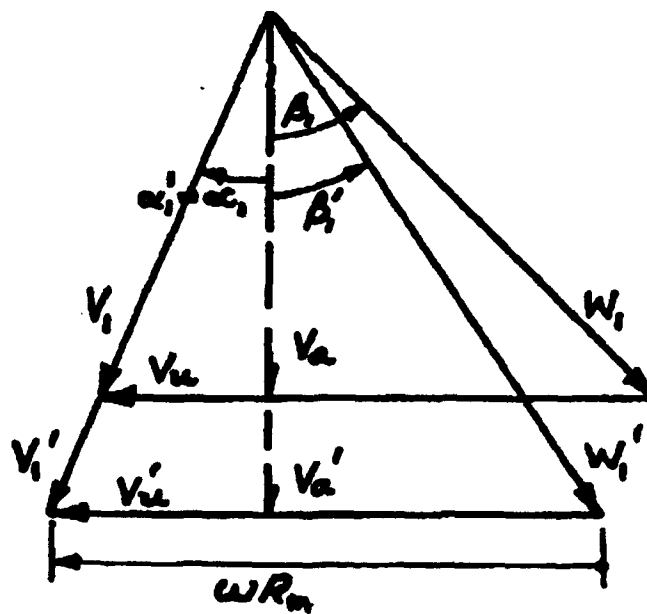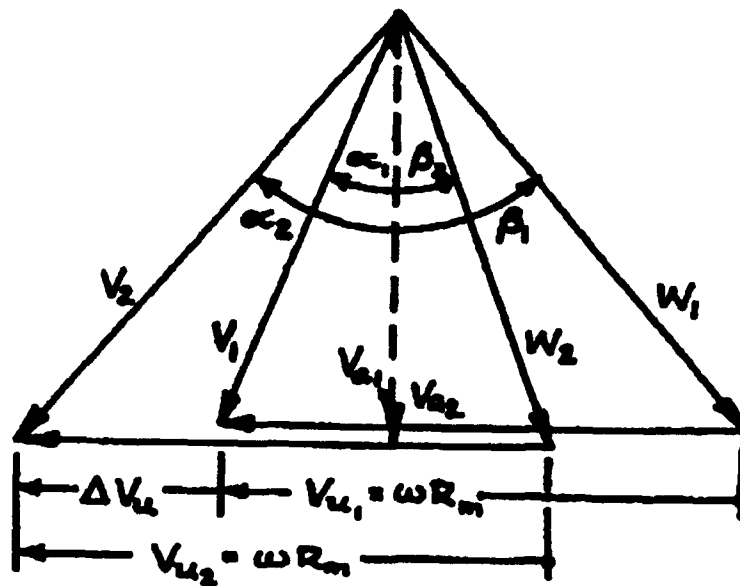
Figure 3. Velocity Diagrams for On-Design (a) and Off-Design (b) Symmetric Blading.

8

TABLE I.   SYMMETRIC BLADING DESIGN FLOW DATA

Rotor (Design Flow Data)

r/r_t	φ (-)	W_1'/U_t	β_1 (°)	$\Delta\beta$ (°)	D_R (-)	σ_R (-)
0.60	0.70	0.86	35.08	27.83	0.250	1.06
0.70	0.68	0.86	37.47	24.54	0.305	0.98
0.80	0.65	0.85	40.00	20.32	0.356	0.92
0.90	0.61	0.84	43.78	15.76	0.402	0.92
1.00	0.54	0.82	48.59	09.63	0.427	0.85

Rotor (Geometric Design Data)

r/r_t	γ (°)	ξ (°)	c/b	t/c
0.60	15.71	40.48	0.333	0.125
0.70	20.30	37.42	0.361	0.098
0.80	25.56	32.54	0.389	0.076
0.90	32.19	26.34	0.417	0.068
1.00	40.96	16.00	0.444	0.062

Stator (Design Flow Data)

r/r_t	V_1/U_t	α_2 (°)	$\Delta\alpha$ (°)	D_S (-)	σ_S (-)
0.60	0.96	31.04	22.57	0.424	1.22
0.70	0.92	35.09	20.12	0.415	1.01
0.80	0.87	39.88	18.60	0.407	0.85
0.90	0.87	39.88	18.60	0.400	0.72
1.00	0.78	52.45	17.36	0.376	0.62

Stator (Geometric Design Data)

r/r_t	γ (°)	ξ (°)	c/b	t/c
0.60	16.07	29.26	0.361	0.065
0.70	21.10	29.28	0.347	0.076
0.80	26.21	31.44	0.333	0.087
0.90	31.20	36.91	0.319	0.100
1.00	34.71	47.58	0.306	0.114

B. LDV INSTRUMENTATION AND DATA ACQUISITION

The LDV system used for this work was a conventional optics, two component system, TSI Model 9100-7. Figure 4 shows the LDV system. The major subsystems include the laser and optics, data acquisition system including the Rotating Machinery Resolver (RMR), data processing system utilizing the PHASE software, traverse table and seeding.

The laser beams were directed through a circular Plexiglas window mounted in a nominally one inch diameter removable plug located in the side of the compressor. The plug was interchangeable with any of the numerous other plugs located in the wall of the compressor test section, allowing for simplified repositioning of the laser window. Figure 5 shows the manufactured optical window and plug dimensions.

1. Laser and Optics

A five Watt Lexel Model 95 argon ion laser was used as the power source. The laser was operated in the multi-line mode and was aligned to a multi-color beam separator after passing through a beam collimator. The beam was split into the green (514.0 nm) and the blue (488.0 nm) wavelengths. Each beam was then further split into two separate beams. A Bragg cell was utilized to allow frequency shifting on one beam in each pair of beams. The frequency shifting was accomplished by use of a TSI Model 9186A Frequency Shifter set at one MHz (one for each color). After passing through the

Figure 4.   Laser,   Optics, and Traverse Table
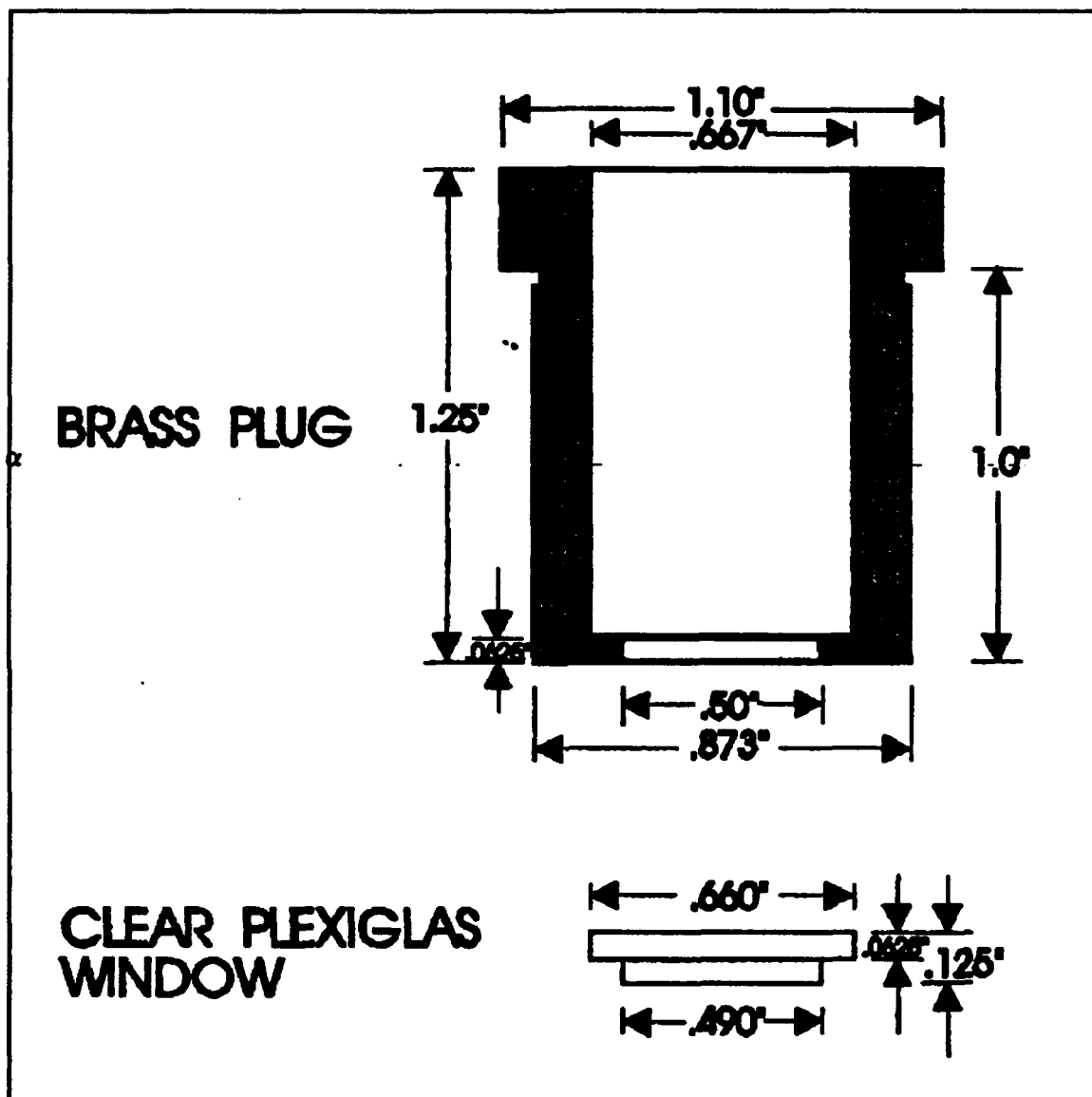
Figure 5.   Laser Optical Window

Bragg cell, a beam stop was then utilized in order to allow only one of the shifted beams through to the beam expander. The beams then passed through a beam expander, which expanded the incident beam diameter by a factor of 3.75. This also decreased the measuring volume length by a factor of 14 and the width by a factor of 3.75, once the beams were refocused. The beam spacing was 0.083 meters and the focal length was 0.762 meters. The final probe volume is 0.00451 millimeters by 2.5 millimeters. Signal-to-Noise Ratio (SNR) was improved by a factor of 50 with the use of beam expanders. The entire system was mounted on a black anodized aluminum base "breadboard", six feet by three feet in extent.

2. Data Acquisition

Scattered light from the seeding was focused by the receiving lens onto the photodetector aperture. In the two component system, a color splitter was used to reflect the green light onto one photodetector and the blue light onto another photodetector. The beams then passed through a field stop to reduce the effects of background flare, extraneous light sources or other laser light reflections. Color filters were also used to further "clean-up" the reflected light. A TSI Model 9165 Photomultiplier (one for each color) was used to convert the optical signal to an electrical signal for processing. The signals were then processed by TSI Model 1990C-1 counter type signal processors, which digitized the

13

doppler frequency. These digital signals were then fed to an IBM PC-AT via a TSI Model MI-990 Multichannel Interface Bus. The laser signal quality was measured using an oscilloscope. Figure 6 shows the LDV signal processing equipment and Figure 7 shows the data acquisition system.

a. TSI Model 1989A Rotating Machinery Resolver

The TSI Model 1989A Rotating Machinery Resolver (RMR) interfaced with the system by providing a Once-Per-Revolution (OPR) signal to precisely correlate the signal to the angular position of the machine. A signal was sent from the signal processor as it recorded velocity data, causing the RMR to latch the angular position of the rotary device at that same instant. The position information was passed along with the velocity data to the computer via the MI-990.

The RMR determined angular position by means of a Phase-Lock-Loop (PLL) method. The circuit "phase-locked" onto the OPR's signal from the rotating machine. It then multiplied the OPR signal frequency by a factor of 3600. This ensured a position resolution of 0.1°. The operator had the choice of phase-lock sensitivity. The four sensitivity settings were 90, 180, 360, and 720 minutes of arc. The RMR triggered within the parameter entered by the operator (i.e., for a sensitivity setting of 90 minutes, the RMR would lock at plus-or-minus 45 minutes of the trigger). As long as the machine remained locked, there were 3600 pulses per

14
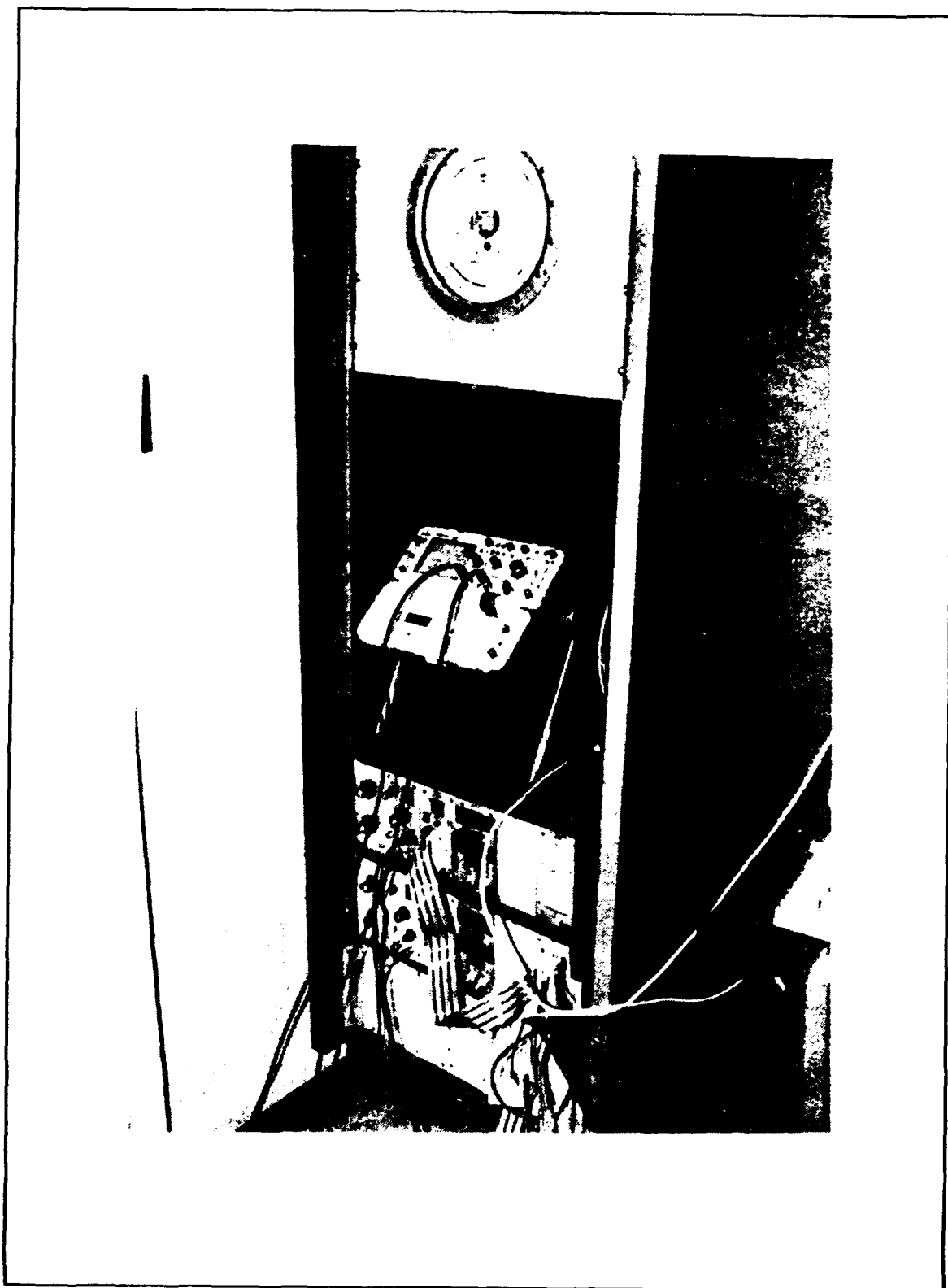
Figure 6.   LDV Signal Processing Equipment

15
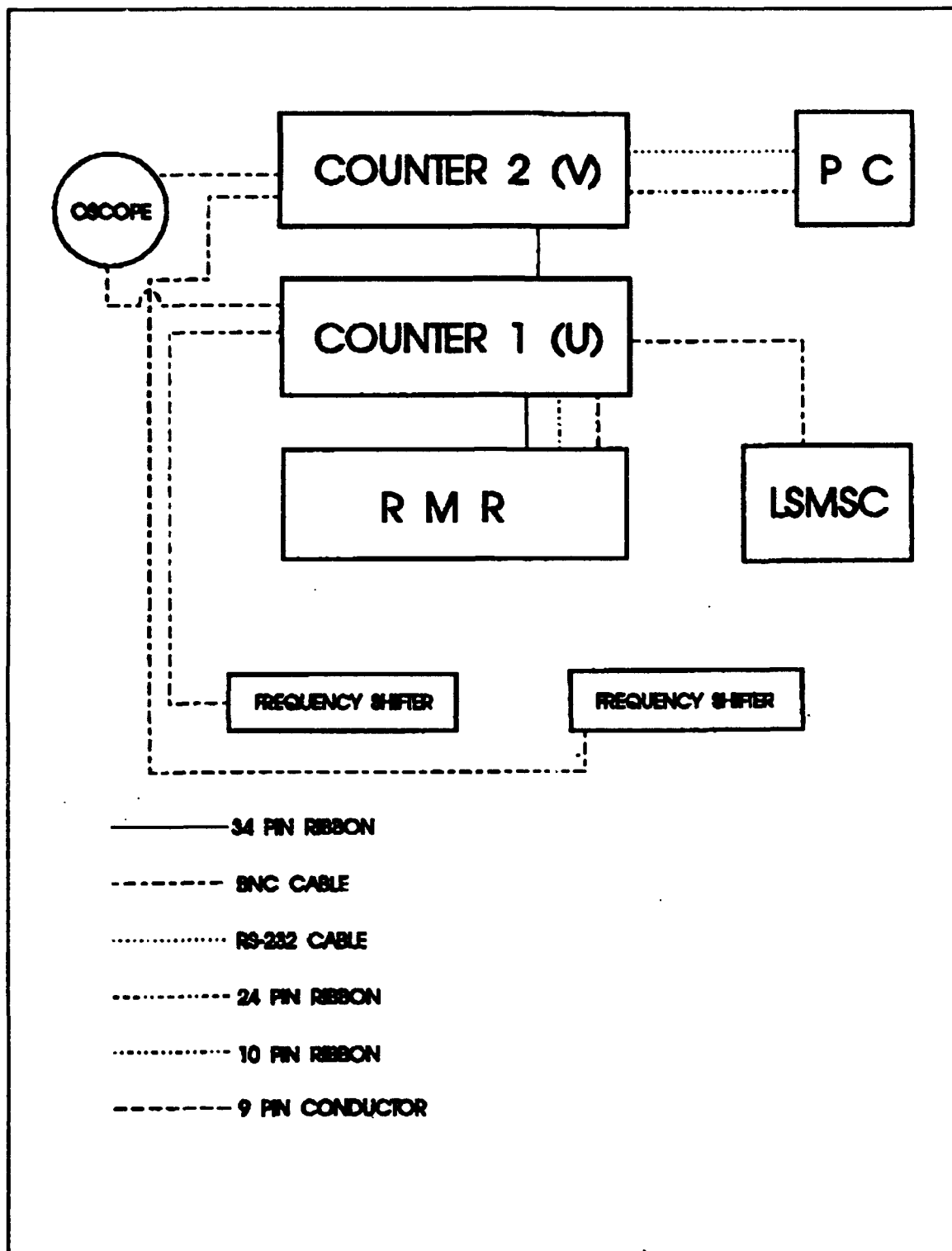
Figure 7.   LDV Data Acquisition System Schematic

revolution. The angular position of the LDV data was then calculated from the number of counts of the phase-locked signal. If the lock was lost, the data was tagged as invalid.

3. Data Processing Using the PHASE Software

The software used was TSI Phase Resolved Software (PHASE). Although the RMR could run with any commercially available data acquisition program, it was designed to be integrated into the PHASE software. The software consisted of three programs: Data Acquisition Program, Statistical Analysis Program, and Traverse Table Program.

a. *Data Acquisition Program*

The Data Acquisition Program controlled the data collection from the signal processors, the RMR phase angle tagging for specific velocity measurements, and the traverse table movement. In addition, PHASE allowed data to be taken in certain bins within the rotating frame. For example, if data were only to be collected in blade passages 10 through 12 in the present LSMSC, the RMR could be programmed to collect data only from 120° (12° per blade passage X 10) to 144° (12° per blade passage X 12). No other measurements would be considered by the software except from this sector.

The PHASE software allowed for the following adjustments:

- I/O Port and Processor Type Selections

17

- Processor Settings

- Optics Configuration

- Experiment Documentation and Units

- Hardware Diagnosis

- Data File Management

- Traverse Table Parameters

- RMR Setup.

b. *Statistical Analysis Program*

The Statistical Analysis Program processed the velocity data into files and statistics. Display choices allowed the selection of either full display of data through the entire rotating frame (or sector chosen) or ensemble averaging over all blade passages or a chosen number of blades. It allowed both tabular and graphical display of the data. It allowed the choice of up to three component statistics, and additional choices of velocity mean, standard deviation, turbulence, skewness coefficient, and flatness coefficient.

c. *Traverse Table Control Program*

The Traverse Table Control Program had seven options to allow the operator to independently control the movement of the table or build a list of coordinate positions which the Data Acquisition System could use for automatically collecting the data. The seven options included:

18

- I/O port selection

- Cylindrical or rectangular coordinate system

- English or metric units

- Reset table to original position

- Position table to a specified location

- Access automatic file menu

- Table immediate halt.

4. Traverse Table

The Traverse Table was a TSI Model 9127 using a Model 9530 controller. The computer control of the table is described in paragraph 3.c. above. For the experiment, the table was traversed manually.

5. Seeding

Seeding is one of the most critical issues in making LDV measurements. Care must be taken that the seeding is of a uniform size, small enough to follow the flow, and able to scatter light sufficiently for detection. The seeding must also be introduced sufficiently far upstream so as not to interfere with the flow.

The seed chosen for the present experiment was olive oil, as it had a uniform size of .9 μm with a standard deviation of .45 μm [Ref 1]. The seed was introduced into the flow approximately three feet upstream of the measurement window, directly behind the inlet guide vanes. The seed particle generator pressure was set at 60 psi and the wand was

inserted approximately three inches into the compressor. The swirl angle in the compressor was approximately 60°, so the seed was introduced at the top of the compressor for measurement at the window (approximately 30° above horizontal).

III. EXPERIMENTAL PROCEDURES

A. LSMSC SET-UP AND PNEUMATIC SURVEY

No changes were made to the blade geometry, inlet screens or inlet bellmouth from those reported by Moyle [Ref. 2]. The areas of the compressor chosen for LDV measurement were at two removable plugs directly upstream and directly downstream of the second stator. The manufactured plug, containing the window, fit into the hole for each of the plugs. The two removable plugs are located at angles of 32° and 31° respectively from the horizontal. As described in Chapter II, seeding was introduced through a wand located at the top of the compressor directly downstream of the inlet guide vane (approximately one compressor diameter upstream).

It was the author's intention to use the automatic pneumatic data collection system to obtain quantities for a reference velocity to non-dimensionalize the data, as well as to map the compressor performance characteristics during the experiment. Appendix I describes the operation of the pneumatic equipment. However, due to unforeseen electrical problems with the Scanivalve Controller, the pneumatic data collection equipment was not available for use during LDV data collection. As a result, a few critical quantities were recorded manually.

For each data run, the following quantities were measured: P_{atmo} (measured in inches of water from a barometer), P_o (measured using a U-tube manometer), P_s (also measured using a U-tube manometer), T_o (using a temperature probe mounted in the freestream approximately five compressor diameters upstream of the test section), and α (using a five hole probe that was manually yaw balanced or null yawed). The data are listed in Appendix III. Only the five hole probe data was used for data reduction.

B. LDV SYSTEM SET-UP AND PRE-RUN VERIFICATION

As mentioned previously, the measurement window areas were approximately 30° above horizontal. The traverse table "breadboard" was designed to tilt a maximum of 11°. Therefore, the traverse table base had to be manually tilted to make up for as much of the difference (30° - 11°) as possible. A wooden platform was built and with the use of the overhead crane present in the laboratory, the entire rear of the assembly was raised and the platform was fitted underneath. Care was taken to square the traverse table to the compressor in order to ensure no radial misalignment of the table. This modification provided an extra 14° of tilt, allowing a total of 25° of tilt when the "breadboard" was fully inclined. The traverse table was not inclined beyond what is described above because any further inclination would be unsafe; not only was there the danger from tilting the

22

table further, but a further inclination would require a greater extension in the Z (approximately tangential - with respect to the compressor) direction of the traverse table, causing a further unsafe shift in the center of gravity of the table. The tilt stressed the Y (approximately radial - with respect to the compressor) direction motor due to the enormous weight of the "breadboard."

The LDV components were set up in accordance with the TSI instruction manuals. The one modification made to the table was a pair of "breadboard" bolts positioned in the front of the Plexiglas cover to prevent it from sliding down and disturbing the photodetectors. Prior to each run, and more often as required, the laser was operationally checked. The "breadboard" was rotated as close to horizontal (11° in the other direction) as possible. The beam crossing was checked with a microscope objective with laser power at 0.5 Watts. Laser output powers in both the shifted and unshifted beams were checked and recorded at 1.0 Watt using a battery powered laser power meter. Laser power was then brought back down to 0.5 Watts and the Bragg cell output was checked visually and adjusted as necessary. After verifying beam output and alignment, the return signal was then checked. Photodetector output was then checked with the alignment eyepiece and usually had to be adjusted with Allen wrenches.

The seeding wand was removed from the compressor and the seed pressure was set at 20 psi. The wand was first placed

horizontally at the beam crossing to check the signal quality of the green beams and then vertically to check the signal quality of the blue beams.

The manufactured plug - without the window - was placed in the chosen measurement hole. The "breadboard" was then rotated to its full tilt limit and the laser beams were sighted and crossed on the side of the manufactured brass plug. The Sony encoder was then zeroed in the Y direction and then moved forward 1.25 inches. (Sony Encoder positions with respect to the compressor and with the laser rig tilted were as follows: X - axial, Y - approximately radial, Z - approximately circumferential). This ensured the beam crossing was now at the inner radial position of the measurement window. The table was then moved as far forward into the compressor as possible. After much trial and error, given the disparity of the angle of the table tilt vs. the angle of the chosen measurement position, it was found to be at an r/r_t of 0.583 at the measurement position downstream of the stator and at an r/r_t of 0.723 at the measurement position upstream of the stator. The beams were then adjusted and manually focused so that all four beams passed through the window. Figure 8 shows the beams when viewed from the exit of the compressor and Figure 9 shows a closeup. This procedure had to be repeated at every window and at every run due to the settling of the traverse table.

Figure 8.   Laser Beam Crossing Inside the Compressor

25

Figure 9. Laser Beam Crossing Close-up

The manufactured plug was then removed and the compressor started. The seeding wand was reinserted into the compressor and the pressure was increased to 60 psi. The signal on both the green and blue channels was verified and the plug was reinserted. The signal was again verified with the window in place prior to taking any data.

The TSI Model 1990 counters were set at four cycles-per-burst and two percent comparison in order to increase the data rate as much as possible, but still ensure a quality signal. Filter settings were set at 1.0 MHz for the low end on the green beams, and 5.0 MHz for the low end on the blue beams. The high filter setting for both pairs of beams was 20 MHz. Gain was set at between 1.0 and 2.0 depending on the survey location. Frequency shifting was set at 1.0 MHz down for both the green and blue beams.

Although seeding was visibly present at the beam crossing for all positions, the data rate was not as high as desired. The software was then set up to take as much data as possible (up to 20,000 data points) within the program time limits (999 seconds). Data were usually taken in the coincidence mode (vs. random mode) to further ensure a clean signal; though near the case wall, random mode was used to try to increase the data rate to usable levels.

As the RMR allowed data to be taken at every 0.1°, data were taken at all 3600 bins around the compressor rotor. Data collection ranged between 1000 points (approximately one data

point every four bins) and 20,000 points (approximately five data points every bin).

With respect to the window, two comments are in order. First, care must be taken when inserting the manufactured plug so as not to disturb the window. The window was not secured in place by anything other than the machined ridge at the bottom of the plug. If the plug was left in place during compressor start-up, the slight pressure rise at start up was enough to pop the plug out of position.

Second, the window was extremely easy to clean. The plug could be removed from the compressor and reinserted without shutting down the compressor. The window was easily popped out and cleaned with lens paper.

C. LDV SURVEYS

As mentioned previously in this chapter, the surveys were conducted at two plug positions. The first immediately downstream of the second rotor, and the second immediately downstream of the second stator. Figure 10 [Ref 6] shows the location of the two plug locations.

1. LDV Surveys Downstream of the Rotor

The LDV surveys conducted downstream of the second rotor were conducted at r/r_t = 0.8889, 0.9167, 0.9444, 0.9722 and 0.9861. The surveys farthest from the case wall (0.8889) were conducted first. Because of the disparity of the angles (25° tilt for the traverse mechanism vs. 31° for the window

28
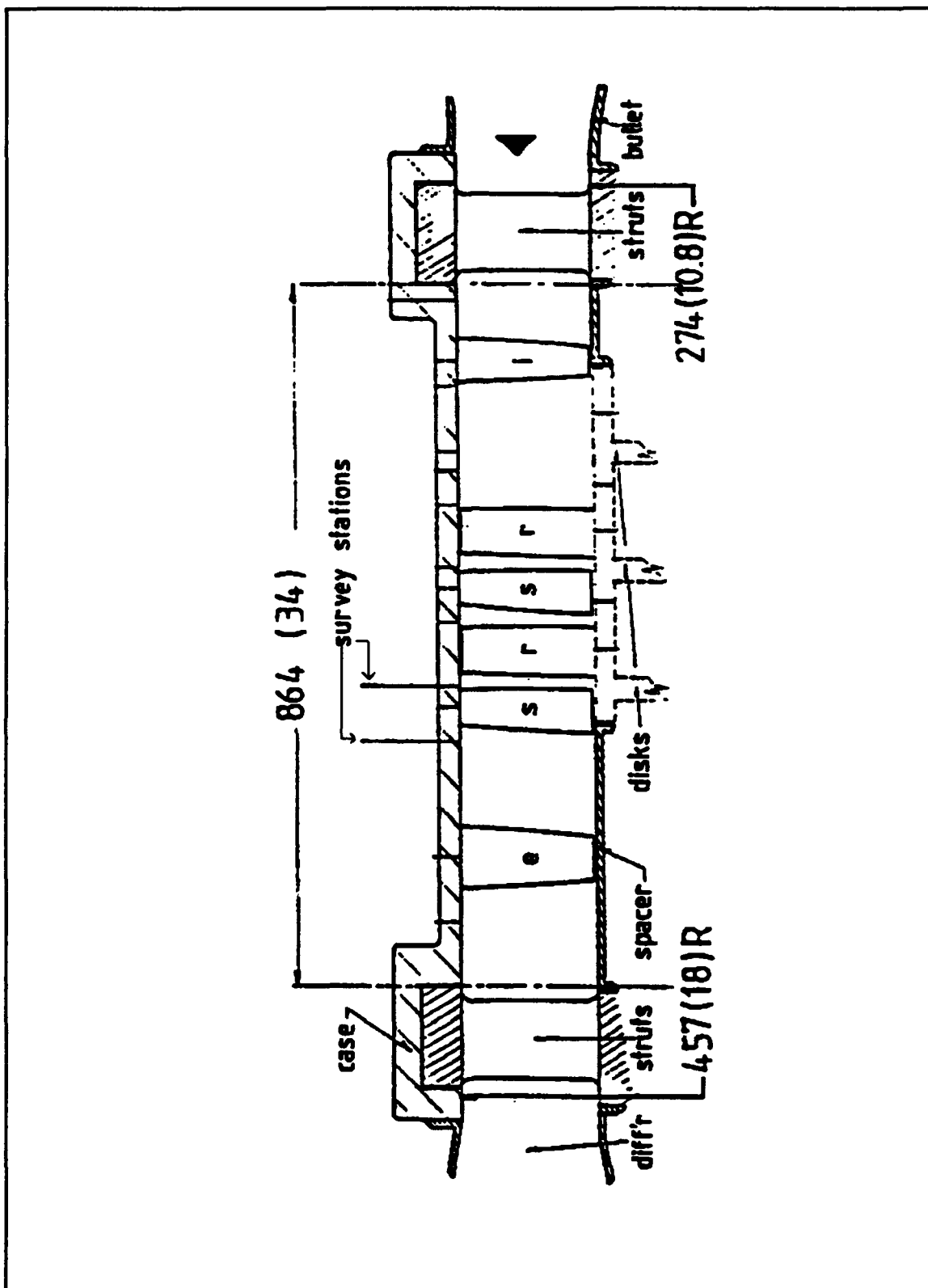
Figure 10.   LDV Survey Positions Relative to the Blading

location), after traversing radially, the traverse mechanism had to be traversed tangentially in order to keep all four beams in position within the window. At the positions closer to the case wall, the amount of tangential traversing required became less. During the course of a survey, no axial movement of the traverse table was permitted.

The taper of the rotor blade, however did not allow each radial position to have the same relative axial position to the rotor blade trailing edge. As a result, additional surveys were conducted 0.125 inches further upstream. Table II is a listing of the radial LDV measurement positions (r/r_t) versus the position (in inches) downstream of the rotor blade trailing edges.

2. LDV Surveys Downstream of the Stator

The LDV surveys conducted downstream of the stator were conducted at normalized radial positions (r/r_t) = 0.8333, 0.9167, 0.9583, 0.9792, and 0.9896. The survey was started at 0.8333 and moved outward towards the case wall. The same angular disparity was present as with the previous surveys, though slightly improved by 1.0° (i.e., the amount of required tangential movement of the laser was less). The same procedures for positioning the laser and setting up the software applied to these surveys as they did previously. Although the RMR was obviously phase-locked to the rotor, the downstream effects of the rotor through a stator passage was

30

TABLE II.   LDV SURVEY POSITIONS RELATIVE TO ROTOR

<u>Rotor</u>

r/r_t (-)	distance (inches)		chord (inches)
.8889	.4219		2.963
.9167	.4531		3.056
.9444	.4375	(.3125)	3.148
.9722	.4844	(.3619)	3.241
.9861	.5000	(.3750)	3.287

Note: Distances listed in parentheses indicate distance from blade trailing edge for surveys taken 1/8 inch upstream of the un-bracketed surveys.

desired.

D. LDV DATA PROCESSING

As described in Chapter II, the software used for data acquisition was TSI's PHASE. After acquisition, each of the files was processed in the statistical analysis portion of the program. Data for each file were acquired over the entire 3600 measurement locations (the complete rotor) and then averaged over one blade passage (ensemble averaged).

The raw data were converted to ASCII files by means of the program PHASRTOA. The files were analyzed by two FORTRAN programs used to reduce the average velocity data of each component (U - circumferential and V - axial) for each survey down to a single value for eventual comparison with the

pneumatic data. Appendix II. lists the programs and
calculations used.

IV. RESULTS AND DISCUSSION

A. OVERVIEW

The results of the study are discussed in the following manner: measurements downstream of the rotor, with individual emphasis first on a comparison with pneumatic data, and then an analysis of the results of each velocity component (circumferential and axial). The flow angle distribution measured downstream of the stator using LDV is compared to pneumatic flow angle measurements.

Compressor runs are denoted by recording the day of the run, the axial position and the radial position. For example, 28 JUN-R-0.9167 indicates a survey taken on June 28, downstream of the rotor at a radial position (r/r_t) = 0.9167.

All data were temporally resolved; i.e., rotor position is reported relative to the probe volume. However, all angles are reported in the absolute frame. Quality of data did vary from survey to survey, with the most consistent data being recorded on the 02 JUL and the worst on 30 JUN. Specifically, for the circumferential velocity component, repeatability was demonstrated and good agreement was found for two or more surveys.

B. LDV DATA DOWNSTREAM OF THE ROTOR

Measurements downstream of the rotor were generally more repeatable and consistent and followed pre-experiment expectations more closely than did data acquisition downstream of the stator.

1. Flow Angle Comparison of LDV vs. Pneumatic Data

Prior to comparison of LDV data to the pneumatic data, all LDV data were ensemble averaged over the thirty rotor passages. In this way, individual blade variations are averaged out. Passage or blade-averaged LDV data (from the three surveys) behind the rotor, in the same axial measurement position as the probe, showed very close agreement with the pneumatic data, with the closest agreement coming in the areas where the most seed was present (the three middle positions; i.e., $r/r_t = 0.9167, 0.9444, 0.9722$). Figure 11 shows the individual LDV results used to make up the average α vs. the pneumatic average α, while Figure 12 shows the LDV average α vs. the LDV average α at the radial position 1/8 inch upstream. A close observation of Figure 11 shows the two positions closest to the casewall for both the 28 JUN and 30 JUN survey to be near identical. However, as noted above, the best data, those taken on 02 JUL, support the pneumatic data, as well as the 1/8 inch upstream data, which show increasing turning angles at the casewall.
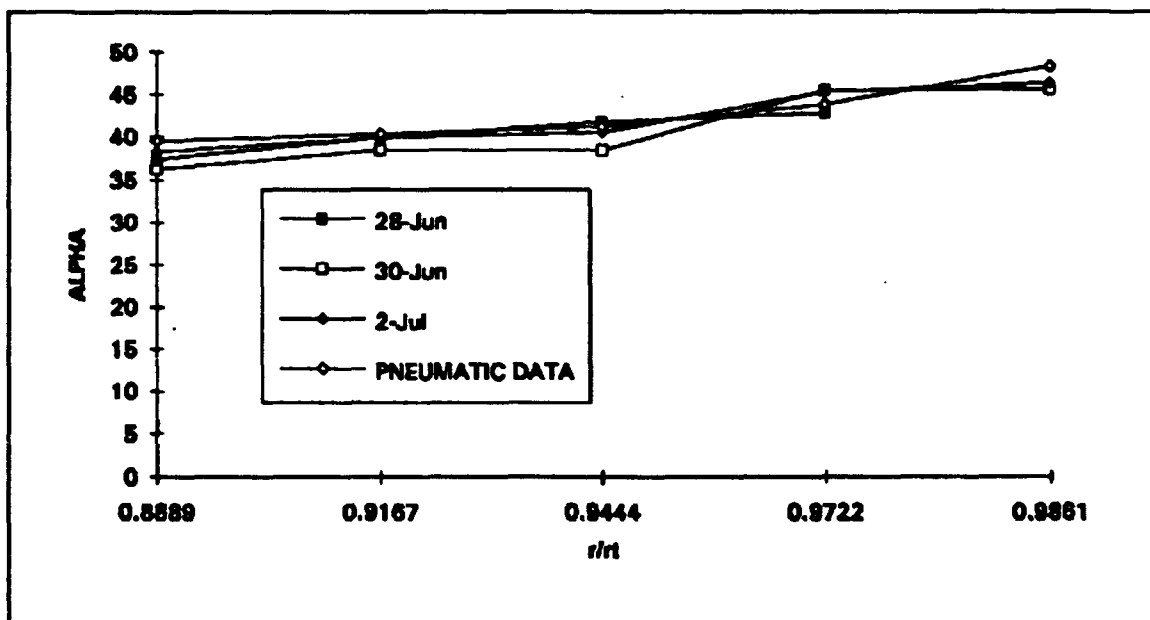
Figure 11. Individual Survey Flow Angle Comparison Behind the Rotor
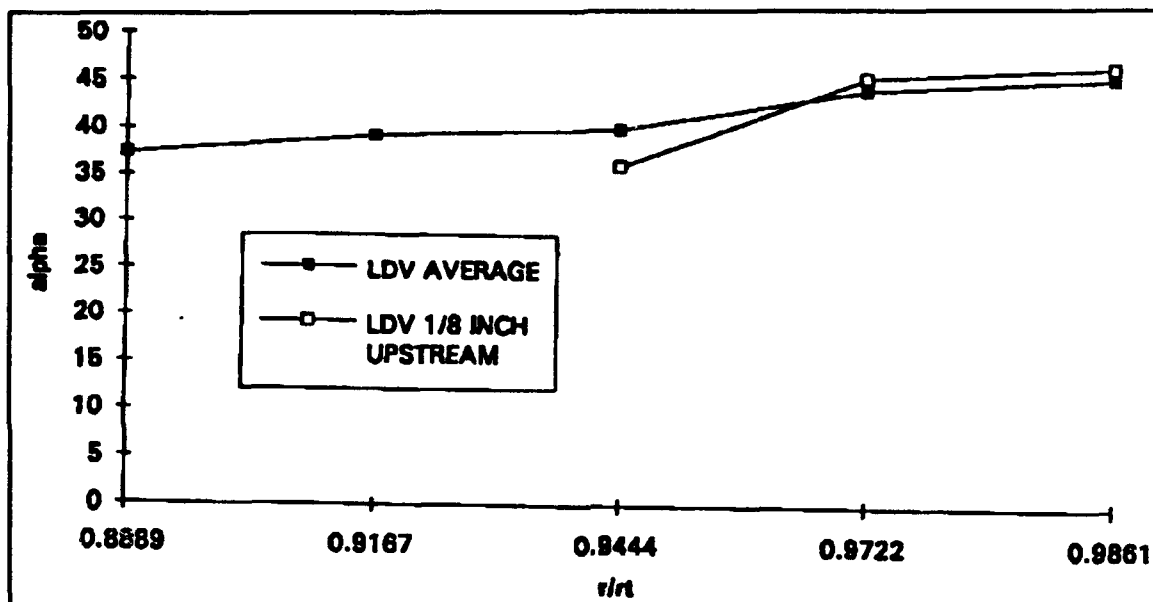
Figure 12.   Flow Angle Comparison Behind the Rotor

An interesting result, however is the lower angle during the survey taken at the 1/8 upstream position at r/r_t = 0.9444. The expected result was a much higher angle due to the physical proximity to the trailing edge of the rotor blade and the lower value is unexplained. Due to problems with the laser, it was not possible to repeat the survey 1/8 inch upstream of the downstream location.

2. Mean Total Flow Vs. Radial Distance

Figure 13 shows the mean total velocity vs. r/r_t for the 28 JUN and 02 JUL. The data were passage-averaged in order to get the time-averaged total velocity magnitude. The mean total velocity drops off towards the casewall. This indicates a boundary layer profile as the surveys progressed towards the case wall.

3. Circumferential Velocity Component

For the mean velocity, data taken on 28 JUN and 02 JUL are considered in an attempt to show experimental repeatability.

a. Velocity Mean

Figure 14 shows the circumferential velocity profiles at r/r_t = 0.8889. They are surprisingly uniform across the wake and show no expected velocity deficit. This may be partly due to the difficulty of seeding at less than an r/r_t of 0.9 due to the axial and radial location of the seeding injection. Averaged mean velocities from survey to survey
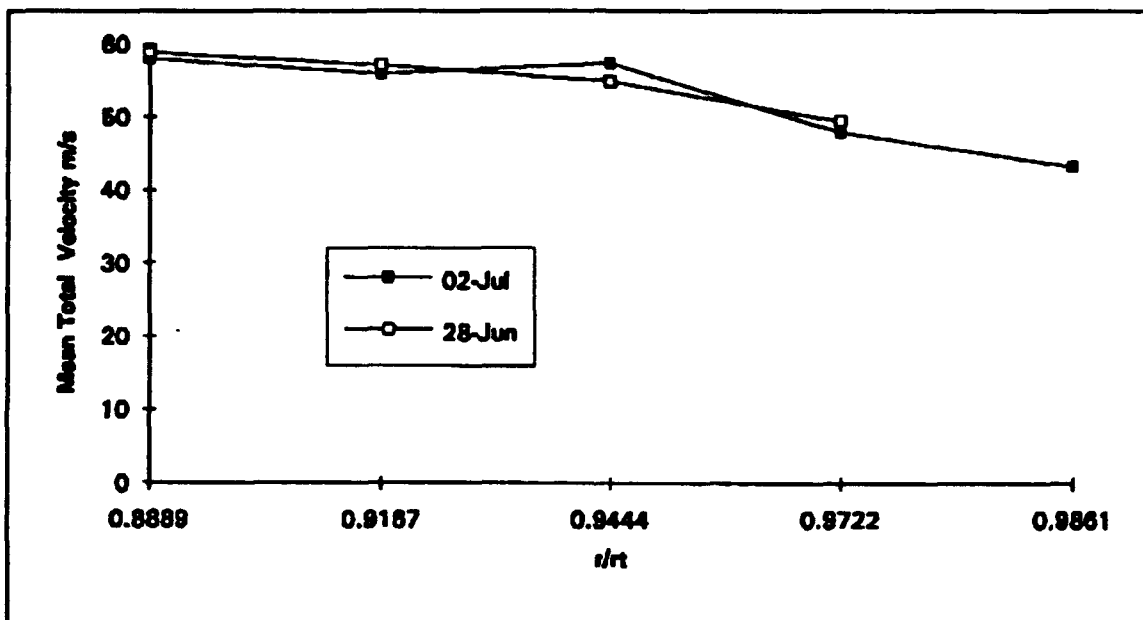
Figure 13. Mean Total Velocity vs. r/r$_t$
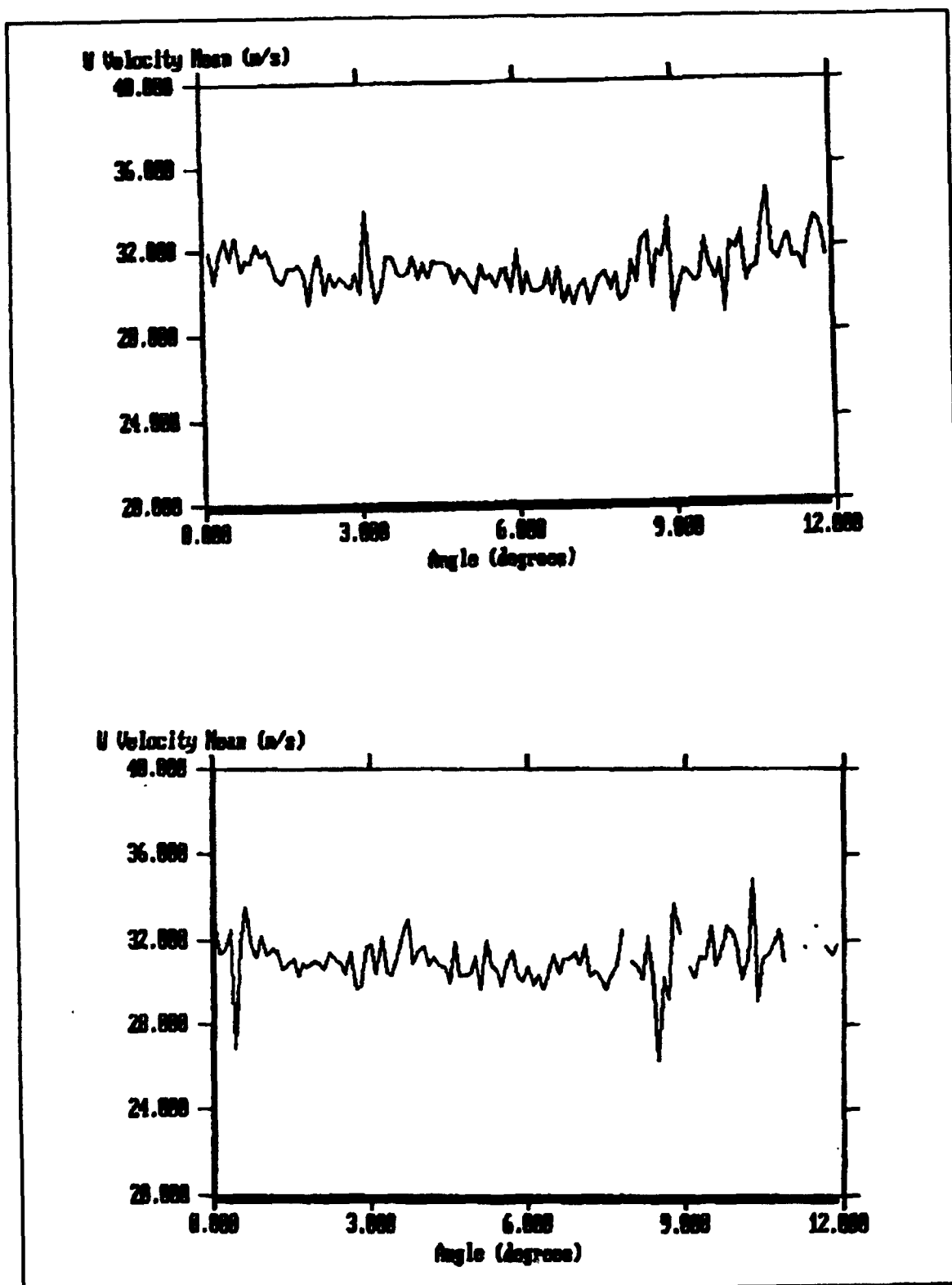
Figure 14.   Surveys 28 JUN-R-0.8889 and 02 JUL-R-0.8889 U
Velocity Mean

39

show a variation of approximately three percent.

The first evidence of a non-uniform velocity profile across the wake occurs at $r/r_t = 0.9167$. A pronounced velocity spike was measured at the ensemble averaged angle of 9.5°, and Figure 15 shows the pronounced velocity spike close to the trailing edge of the blade. Figure 15 also shows the approximate location (7.5°) of the blade trailing edge in comparison to the velocity profile. The figure also shows the suction side and pressure side of the blade, as well as direction of rotation. At $r/r_t = 0.9444$ the velocity peak is slightly higher by about two percent for each _individual_ survey. Figure 16 shows the visible peak for both surveys. In addition to being slightly higher, the peak has moved slightly from 9.5° to approximately 10°.

Also at $r/r_t = 0.9722$, the velocity spike has increased and moved to the right. This movement of the peak away from the blade trailing edge is due to increased axial distance downstream of the trailing edge and due to blade twist. Figure 17 shows an increased velocity gradient prior to the spike vs. that of the previous r/r_t position. The mean flow variation across the passage has also increased, which could be an indication of proximity to the endwall boundary layer and tip leakage flow.

The data at $r/r_t = 0.9861$ (Figure 18) shows a decrease in the velocity. The velocity profile across the
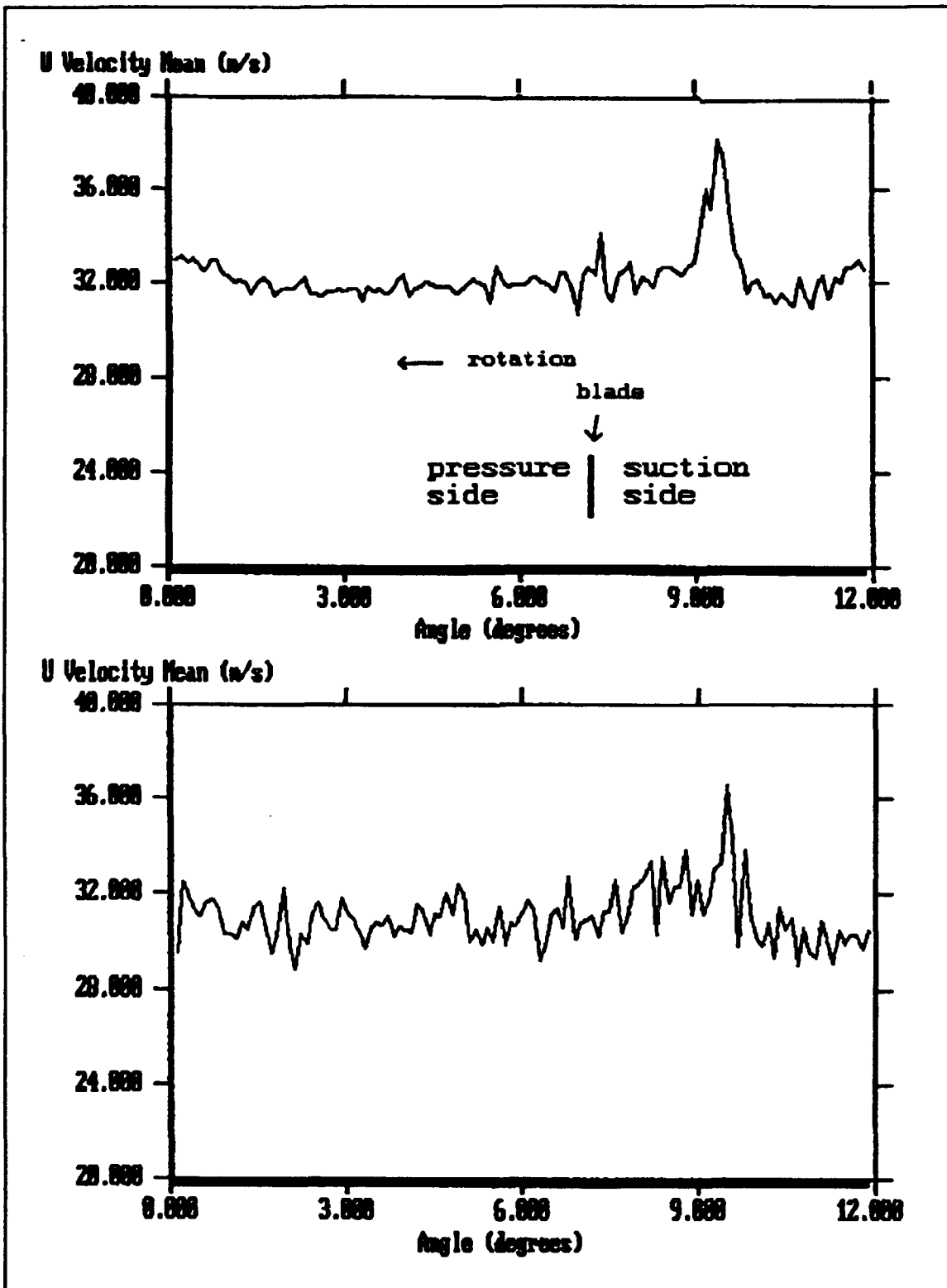
Figure 15.   Surveys 28 JUN-R-0.9167 and 02 JUL-R-0.9167 U
Velocity Mean
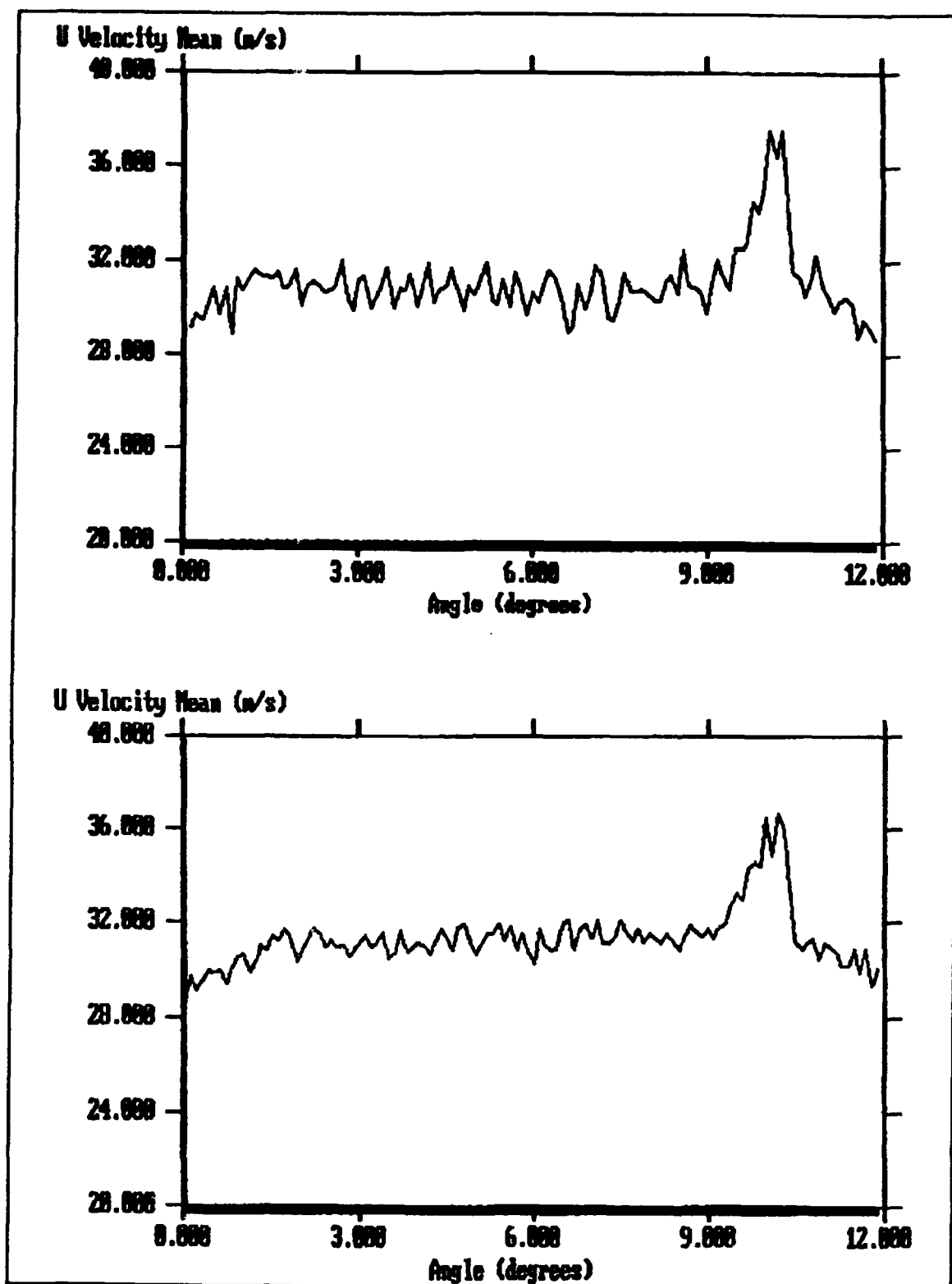
Figure 16.   Survey 28 JUN-R-0.9444 and 02 JUL-R-0.9444 U
Velocity Mean
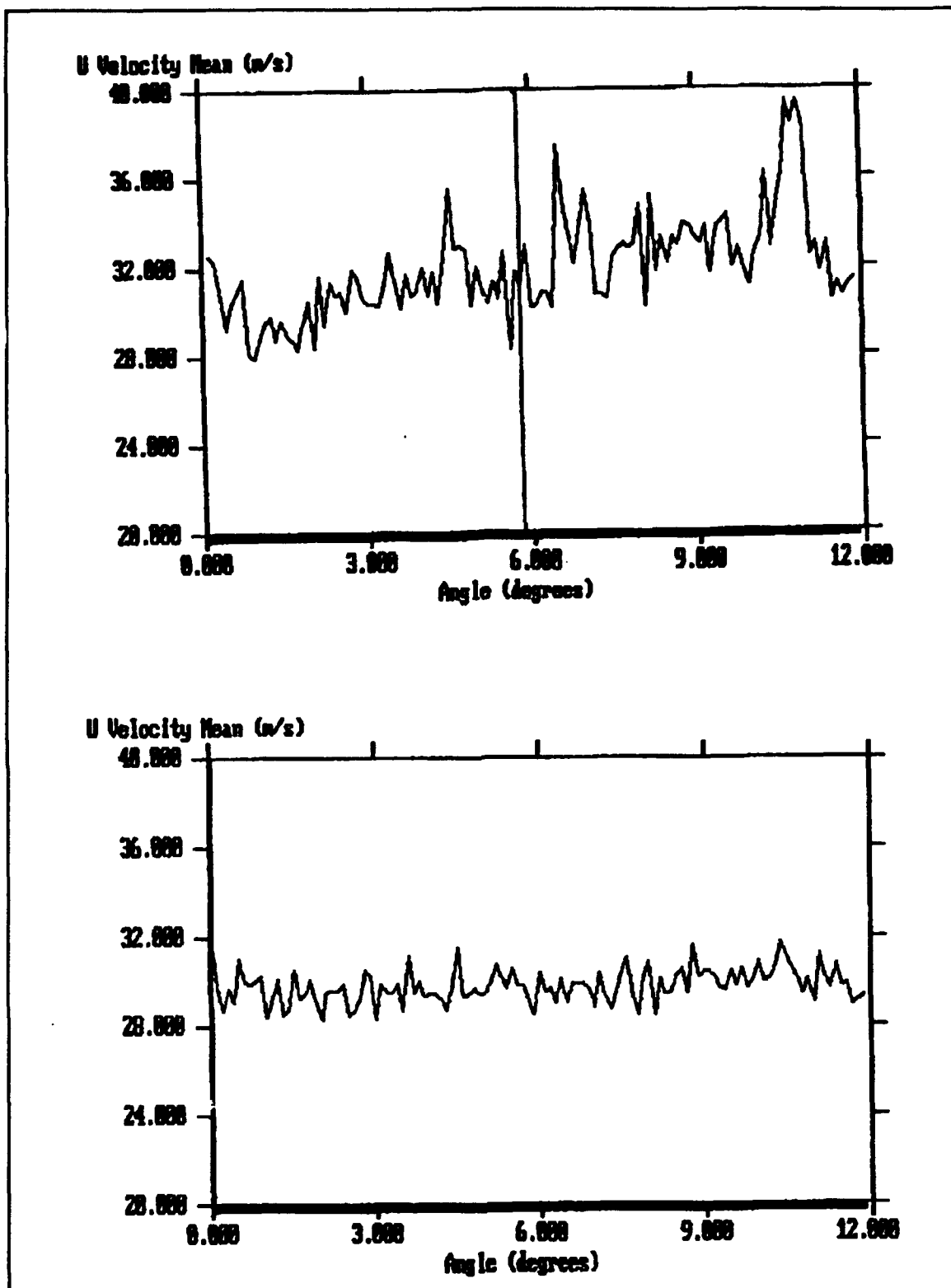
Figure 17.   Survey 28 JUN-R-0.9722 and 02 JUL-R-0.9722 U
              Velocity Mean
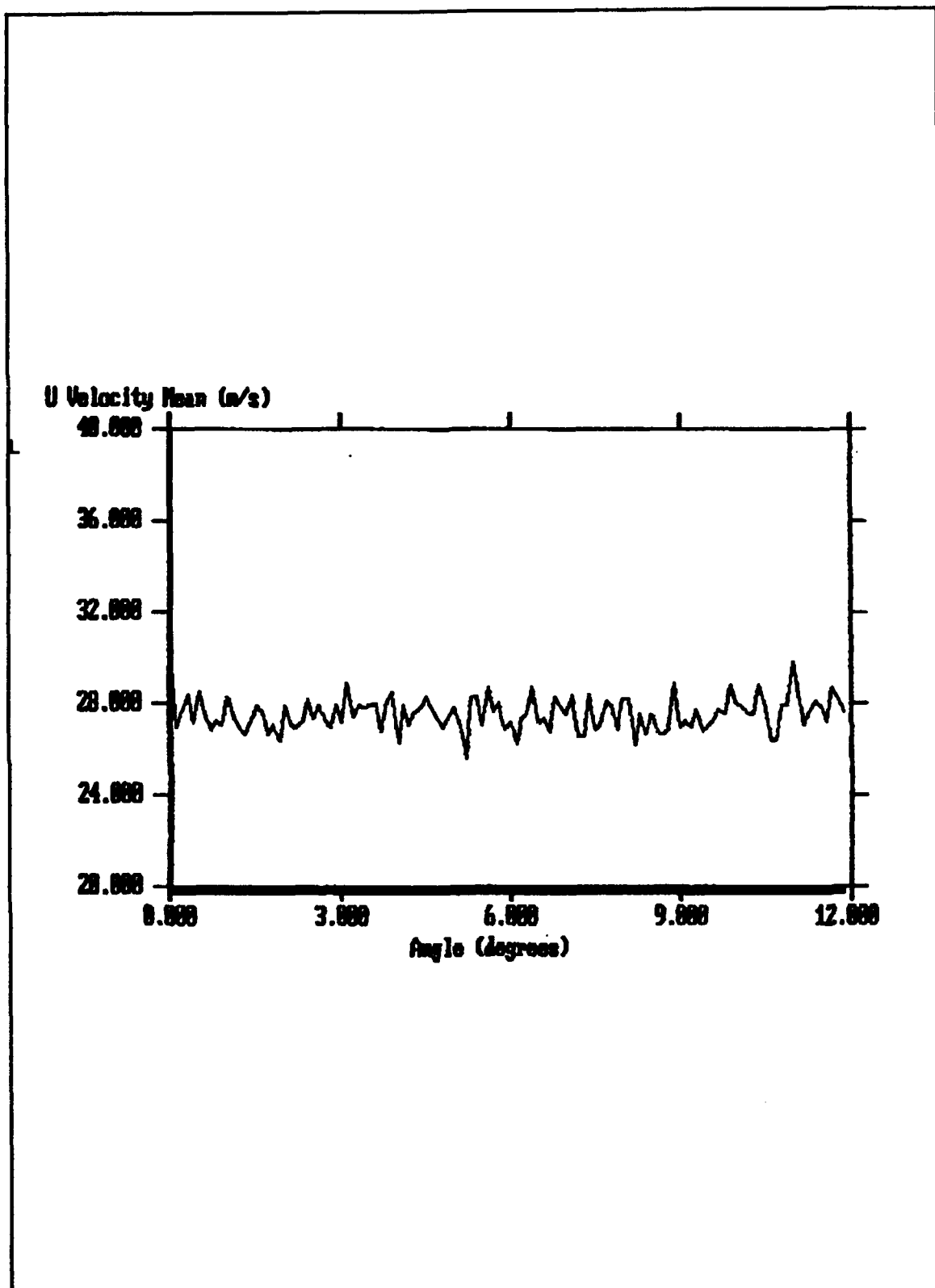
Figure 18.   Survey 02 JUL-R-0.9861 U Velocity Mean

blade passage is almost uniform. The lack of a wake profile is probably caused by endwall boundary layer mixing. Unfortunately there was no signal present for a 28 JUN-R-0.9861 survey, so only the results from 02 JUL are presented.

b. Flow Unsteadiness

The data points taken in each individual survey were analyzed to examine the degree of flow unsteadiness. Figures 19 - 23 show the percentage of flow unsteadiness at all radial positions measured on 02 JUL. Note that the flow unsteadiness spike at the mean velocity increase near the 9° position on graphs for low r/r_t values. At higher values of r/r_t the flow unsteadiness appears to increase in level and this is once again due to the tip leakage and endwall boundary layer flows, which are inherently more unsteady. All surveys shown for 02 JUL were ensemble averaged over 20,000 data points.

4. Axial Velocity Component

A most expected result came about with the analysis of the data for the axial component. Figures 24 - 28 show the results starting with the smallest r/r_t for the data taken on 02 JUL. Specifically, in the surveys at $r/r_t = 0.8889$ and 0.9167, there is a pronounced velocity drop at the ensemble averaged angle of around 10°. As with the velocity spike in the circumferential velocity component, the velocity drop
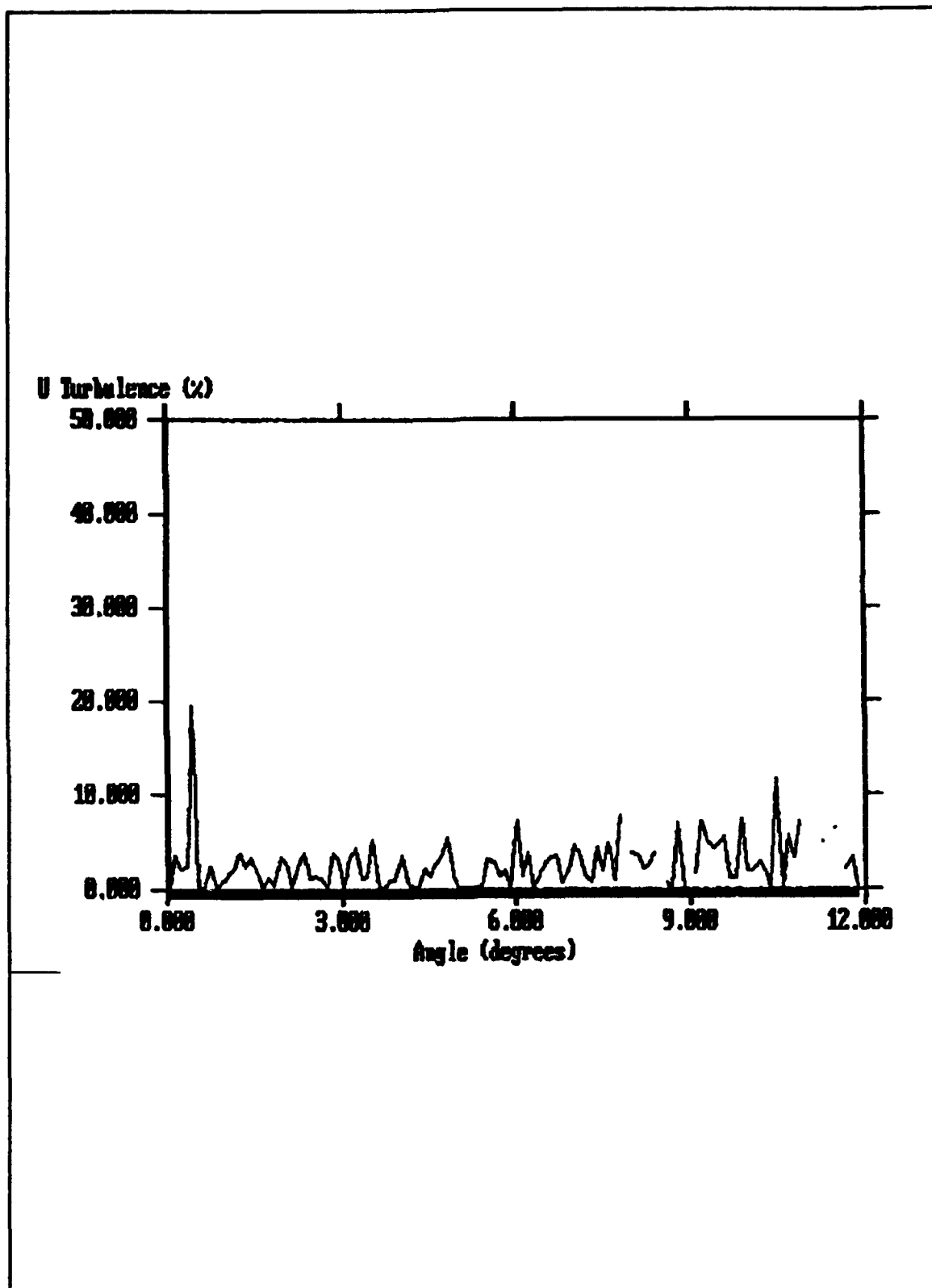
Figure 19.   Survey 02 JUL-R-0.8889 U Turbulence

46
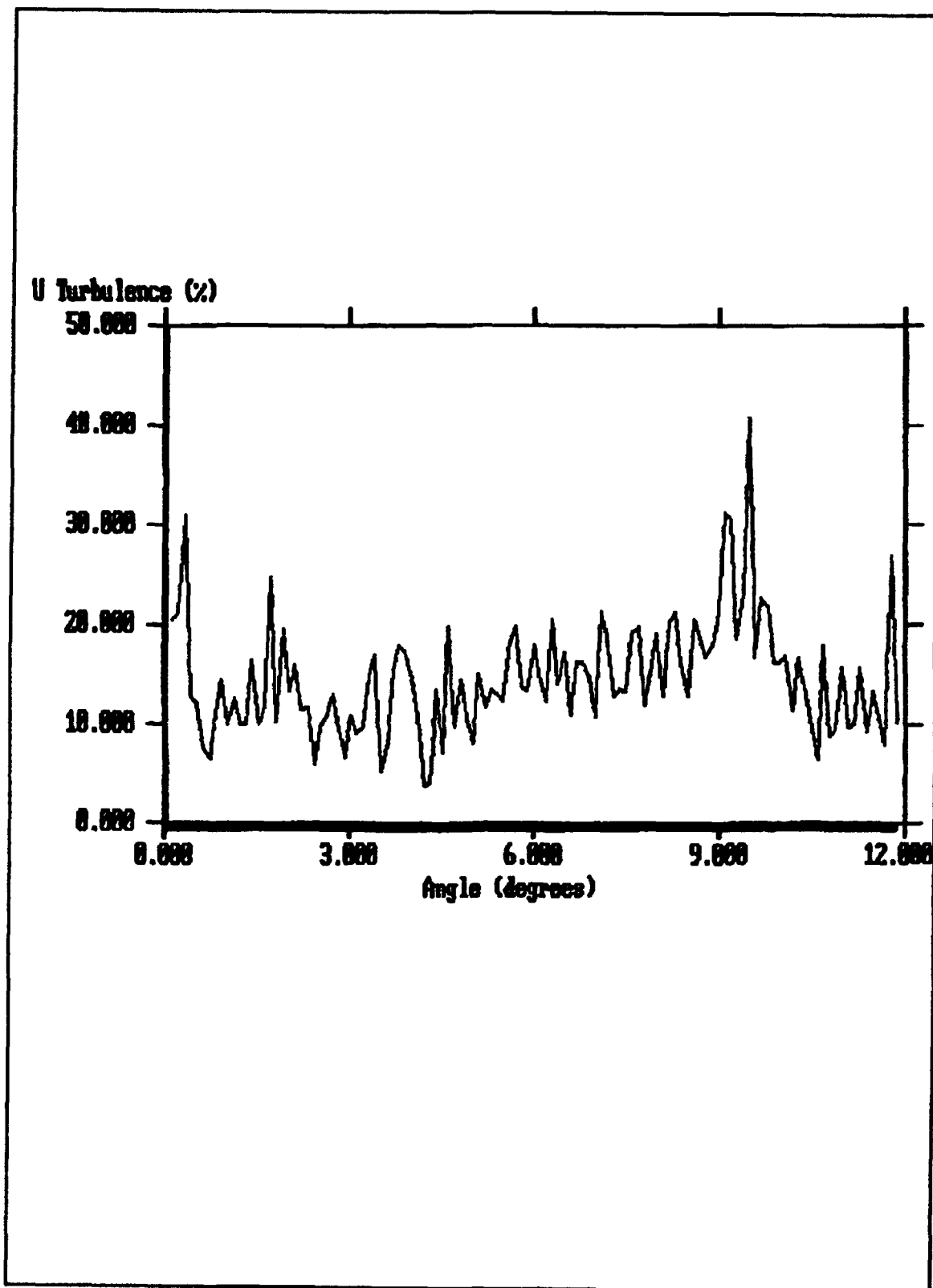
Figure 20.   Survey 02 JUL-R-0.9167 U Turbulence

47
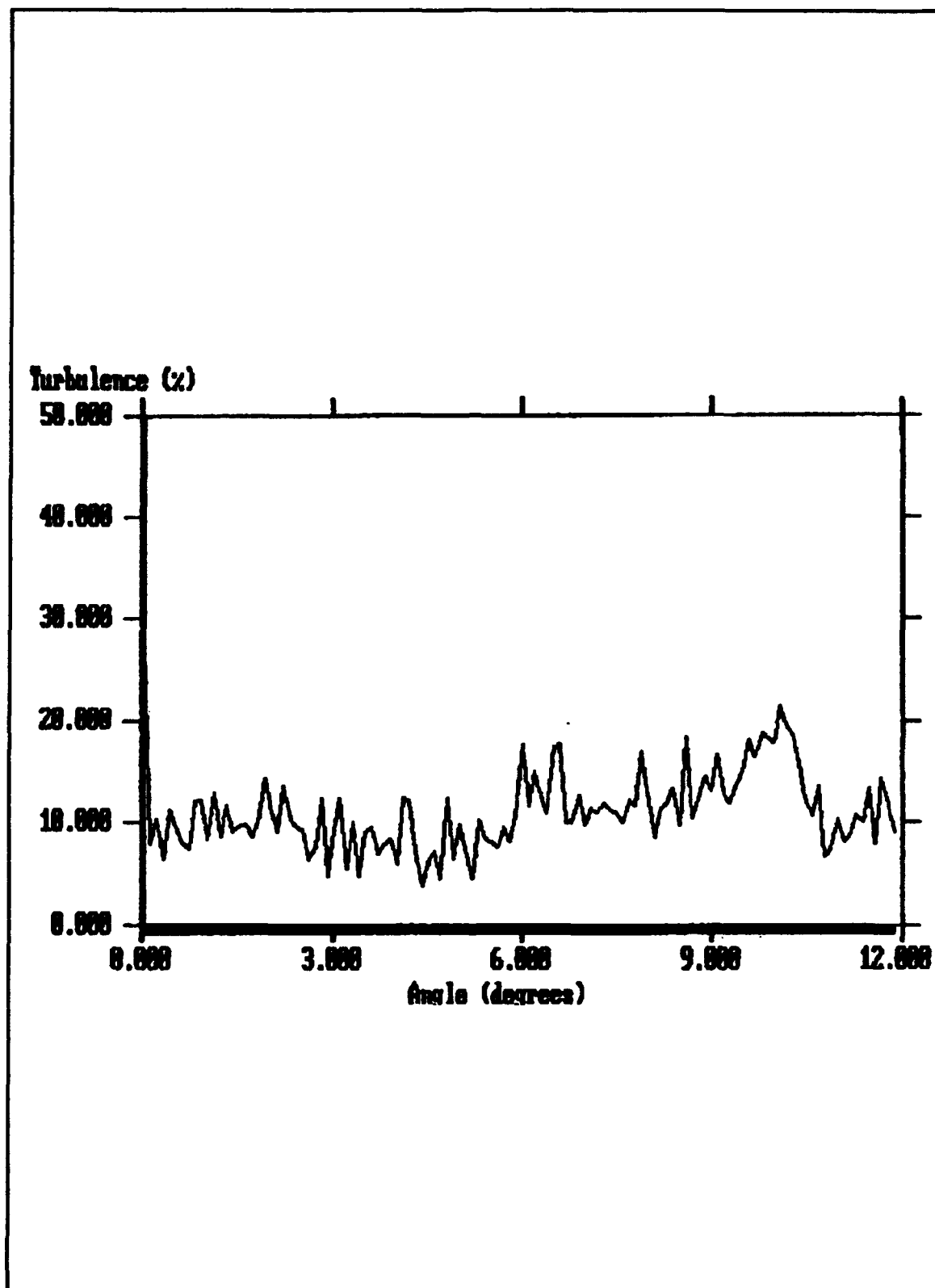
Figure 21.   Survey 02 JUL-R-0.9444 U Turbulence

48
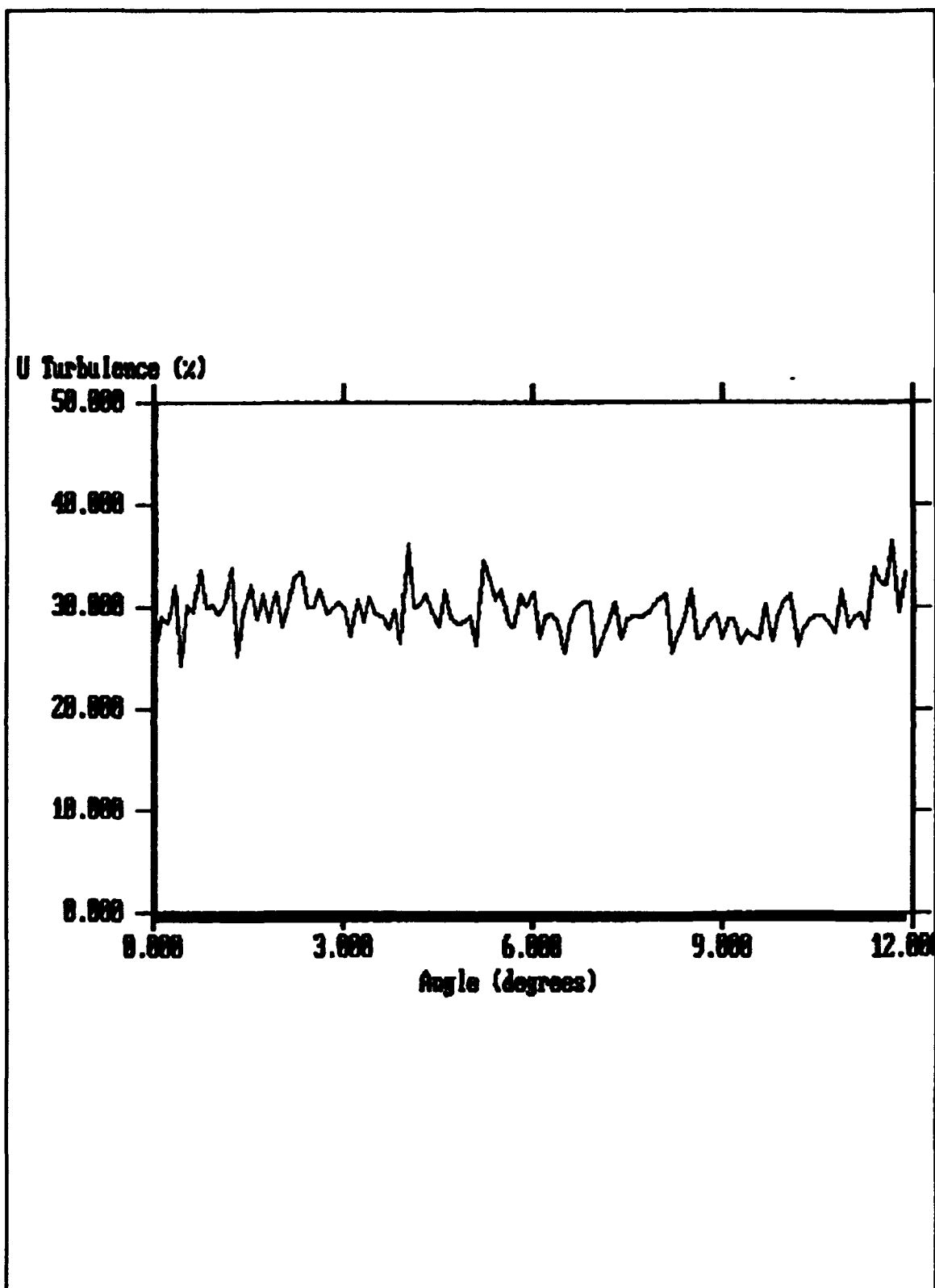
Figure 22.   Survey 02 JUL-R-0.9722 U Turbulence

49
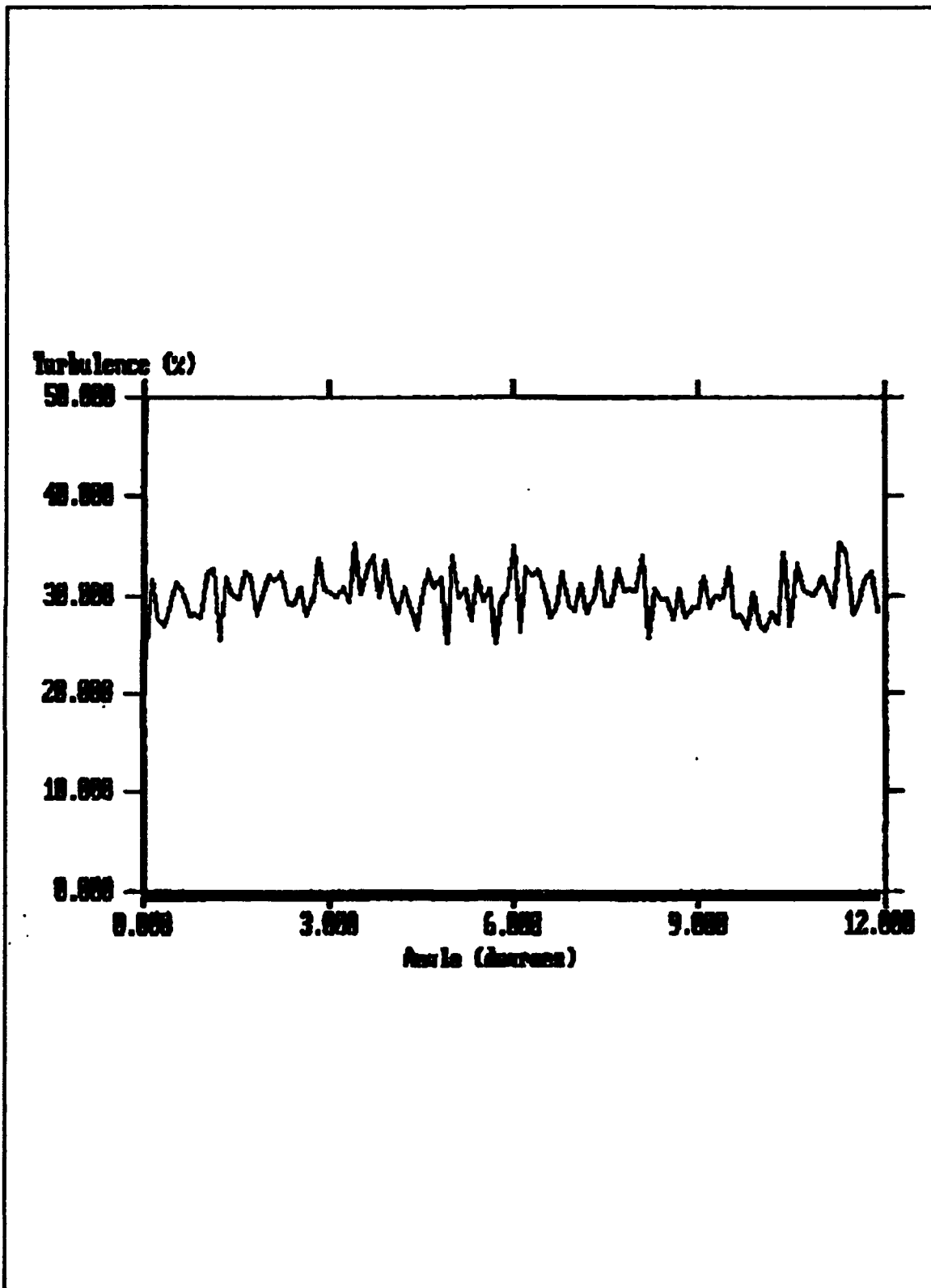
Figure 23. Survey 02 JUL-R-0.9861 U Turbulence

50
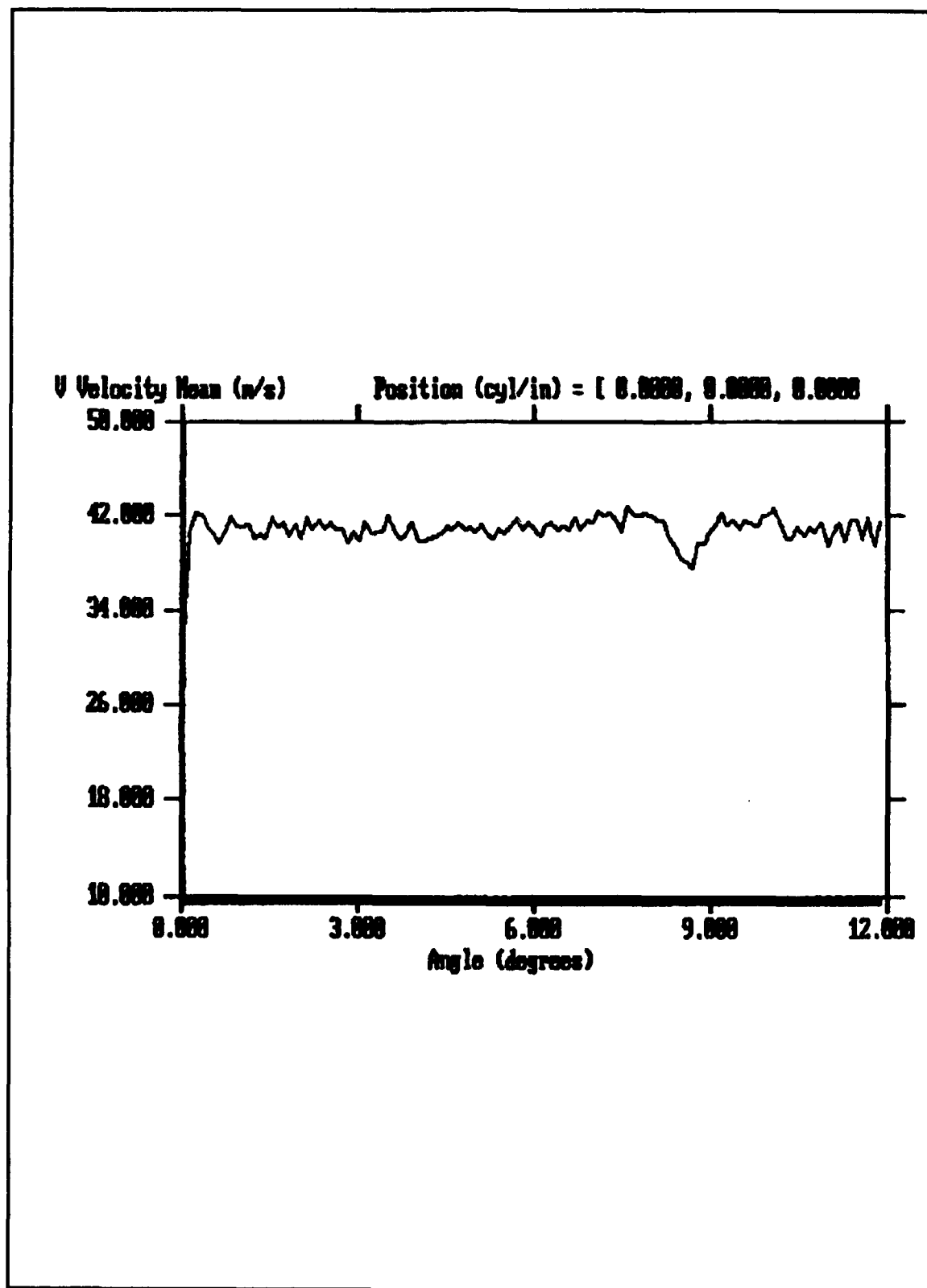
Figure 24.   Survey 02 JUL-R-0.8889 V Velocity Mean

51
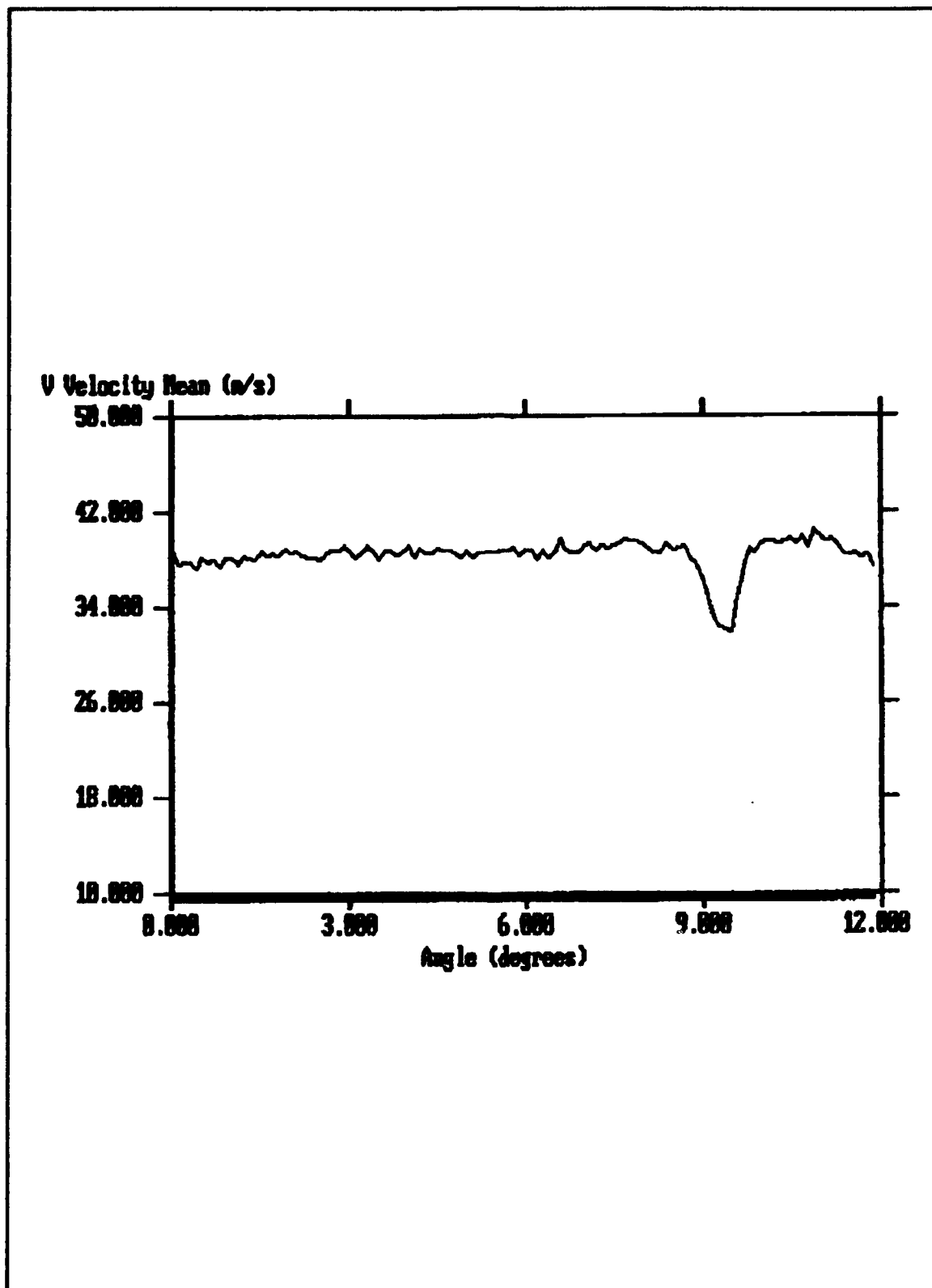
Figure 25.   Survey 02 JUL-R-0.9167 V Velocity Mean

52
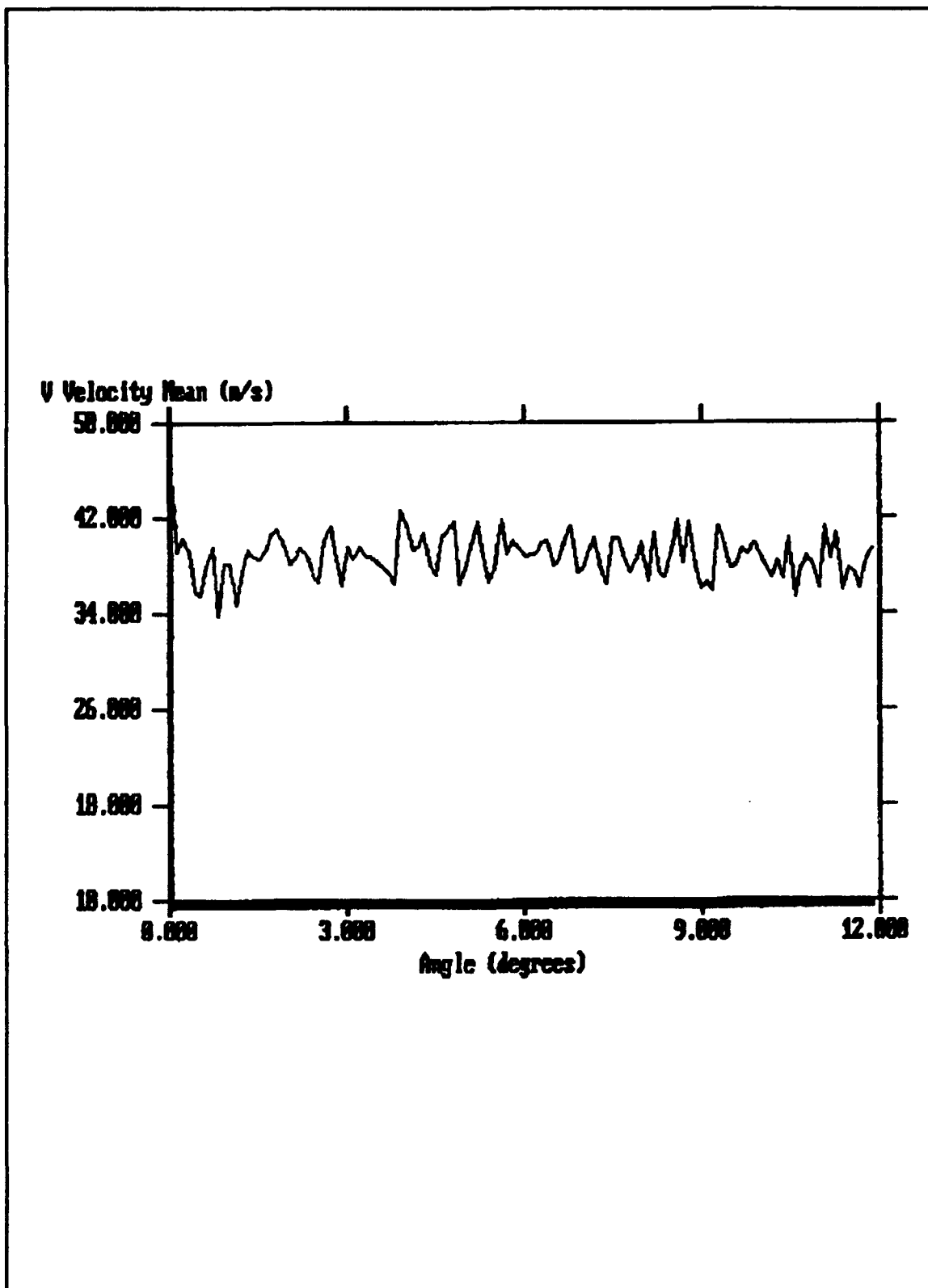
Figure 26.   Survey 02 JUL-R-0.9444 V Velocity Mean

53
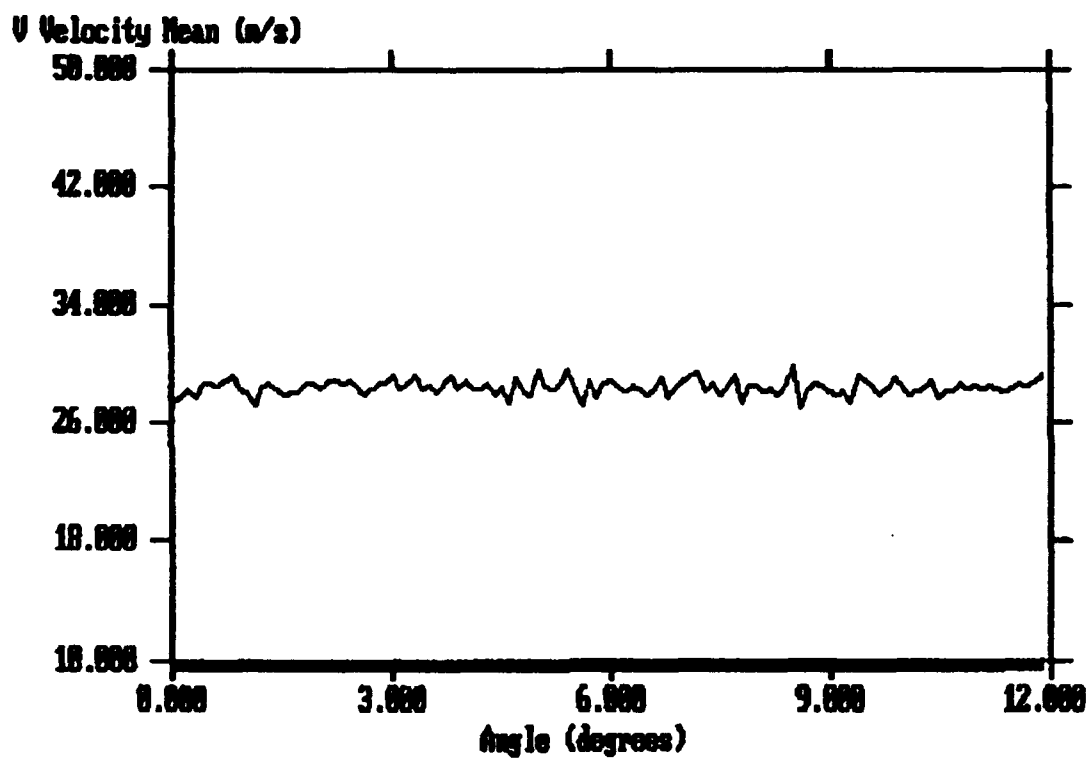
Figure 27.   Survey 02 JUL-R-0.9722 V Velocity Mean
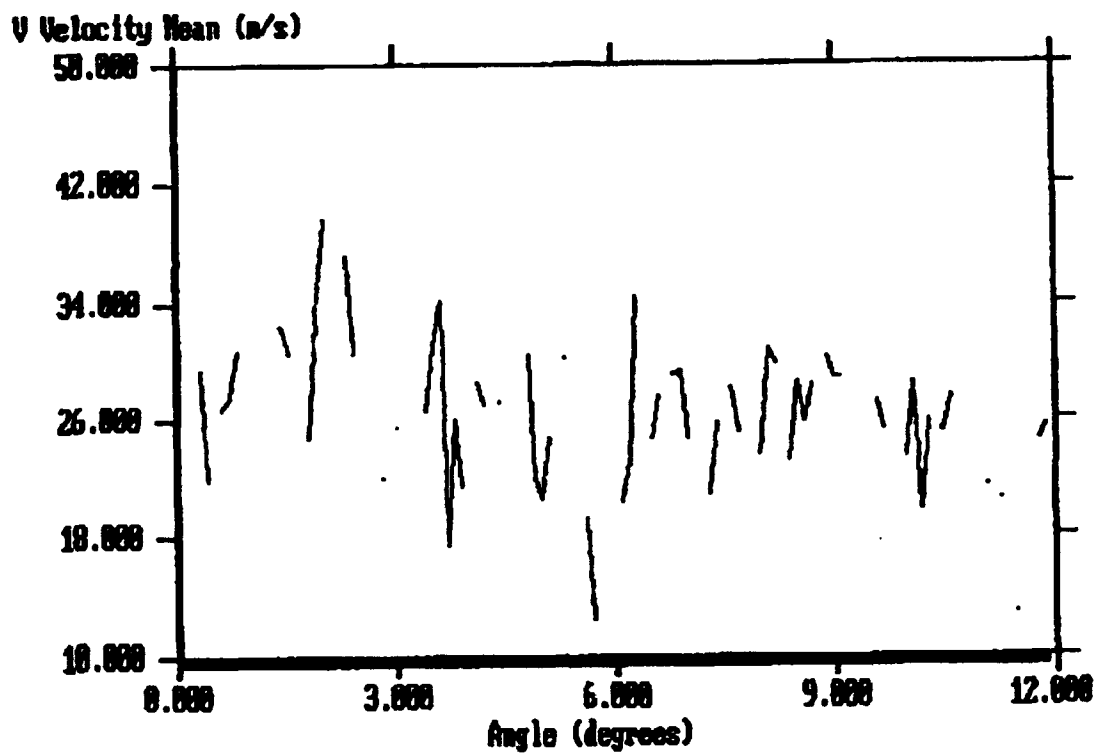
Figure 28.   Survey 02 JUL-R-0.9861 V Velocity Mean

55

appears to move to the right with increased r/r_t.

5. Data 1/8 Inch Upstream

Figures 29 - 31 show the comparison of axial and circumferential data at the survey position 1/8 inch upstream. As noted before, the survey was unfortunately unable to be repeated. The data are included for comparison purposes only. The first two figures clearly show the position of the wake, and at r/r_t of .9861 (Figure 31), the endwall boundary layer and tip leakage flow has mixed out the wake.

C. LDV DATA DOWNSTREAM OF THE STATOR

Five separate radial positions were measured, at one axial and circumferential location. The ensemble-averaged rotor profiles were smeared out to a uniform flow downstream of the stator. Only averaged LDV flow angles vs. pneumatic flow angles could be reported for the stator. Since all measurements were indexed to the rotating frame of reference, all LDV data behind the stator were ensemble averaged over the thirty rotor passages. Averaged LDV data (from two surveys) behind the stator showed close agreement with the pneumatic probe data, though not nearly as close as behind the rotor. Figure 32 shows the plot of the angle vs. r/r_t in the absolute frame, and Figure 33 shows the individual results used to calculate the average.
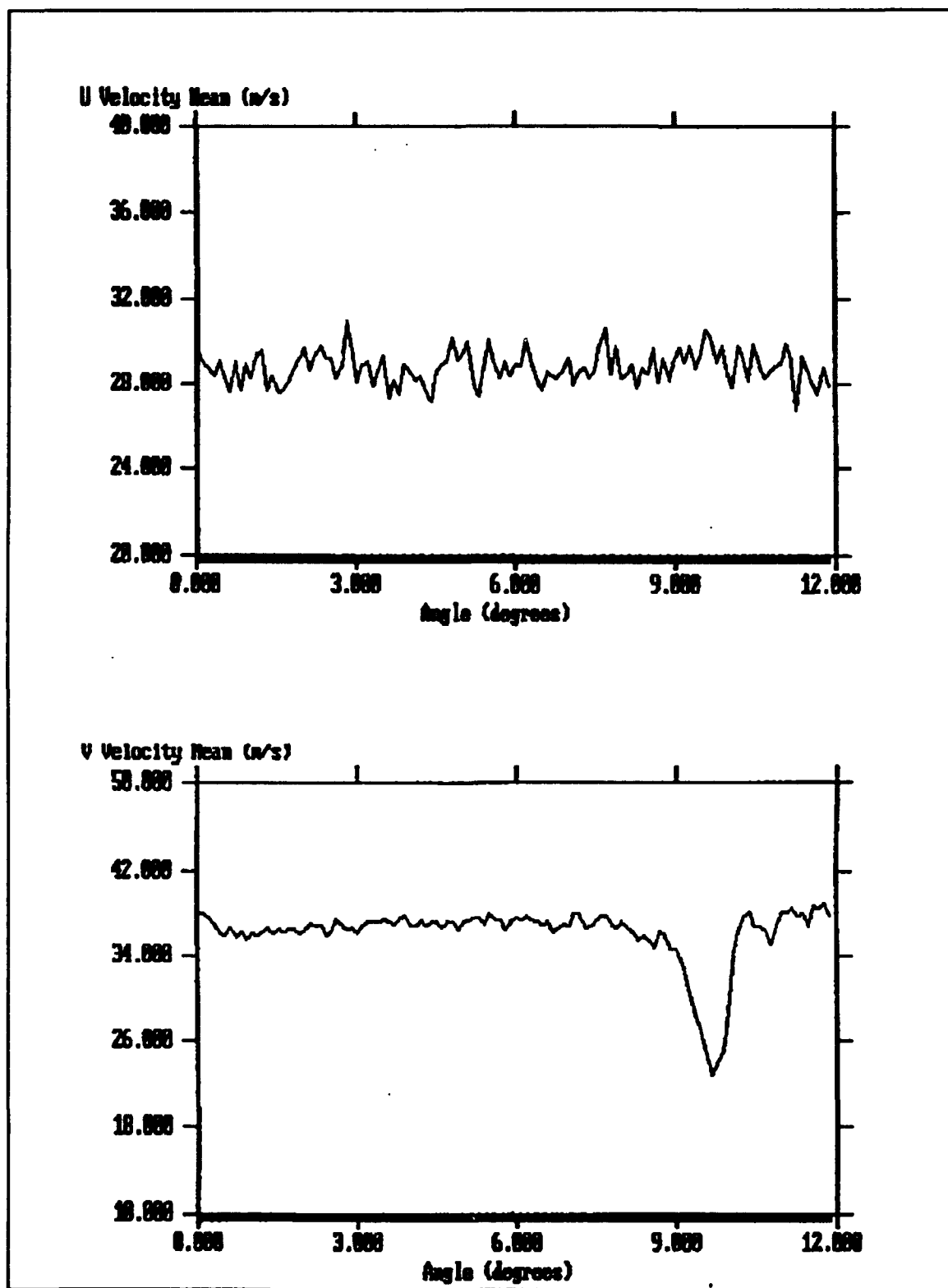
Figure 29.   Surveys 15 JUL-R-0.9444 1/8 Inch Upstream
U and V Velocity Mean
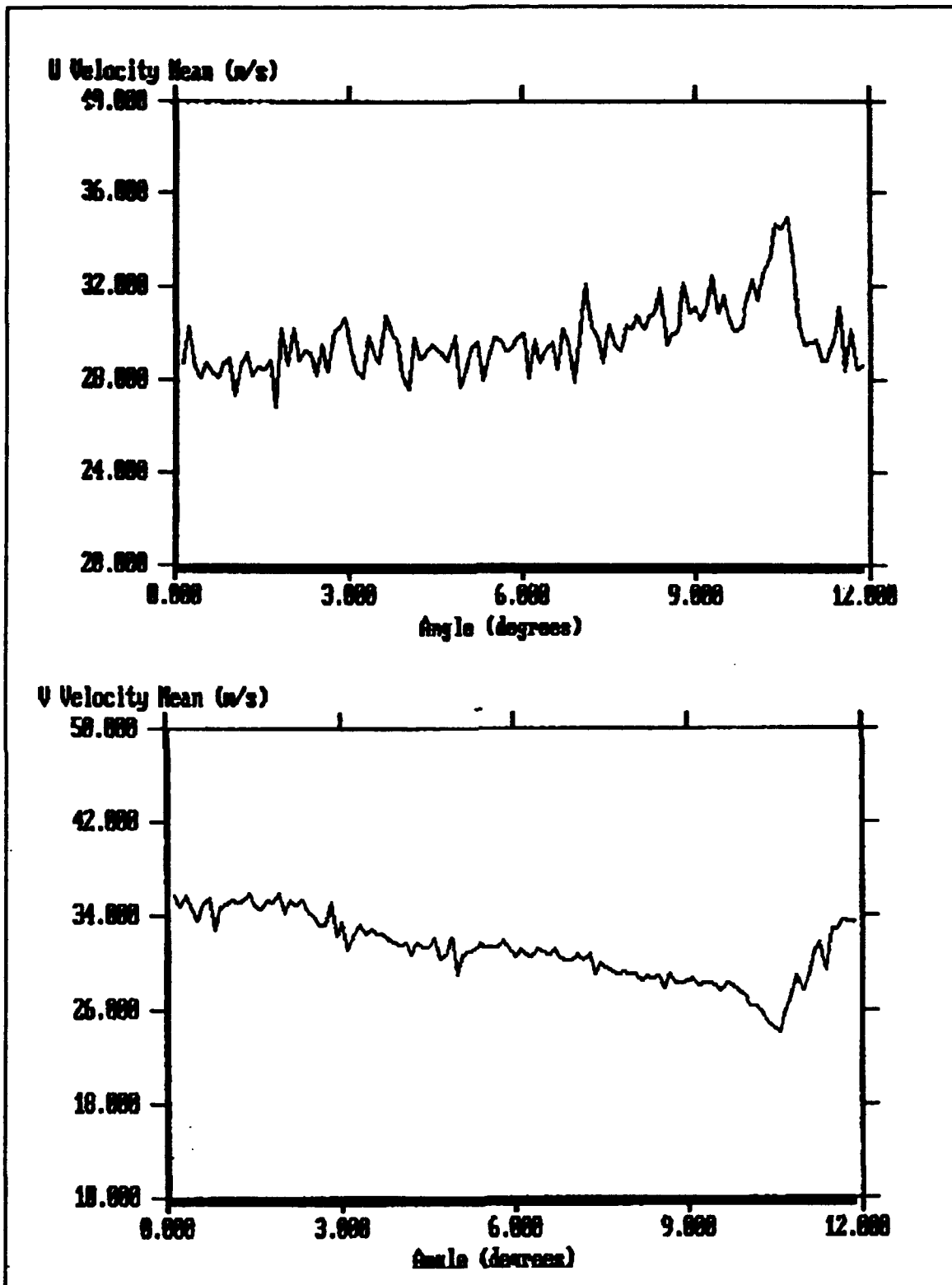
Figure 30.　Surveys 15 JUL-R-0.9722 1/8 Inch Upstream
U and V Velocity Mean
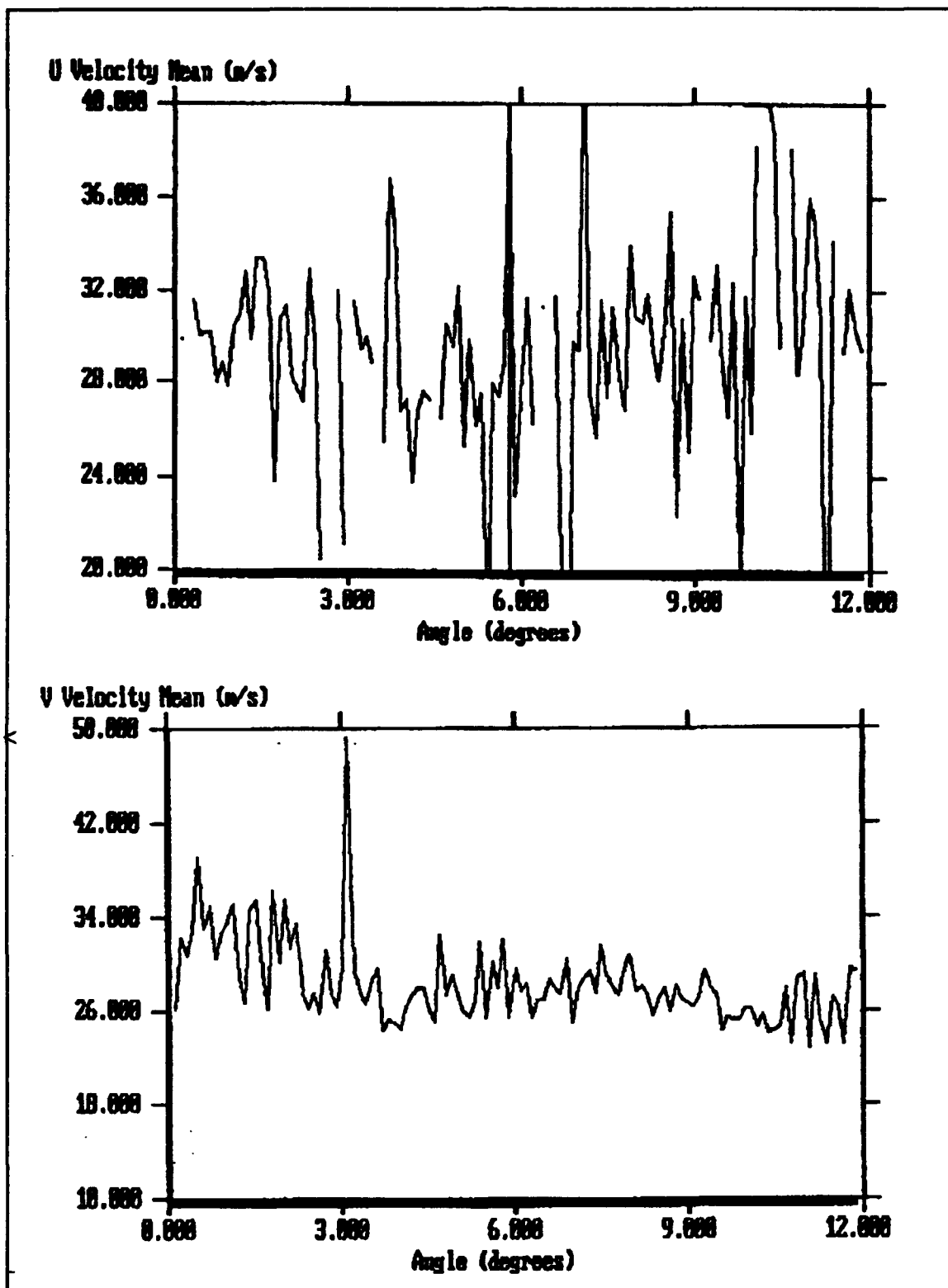
Figure 31.   Surveys 15 JUL-R-0.9861 1/8 Inch Upstream
U and V Velocity Mean

59
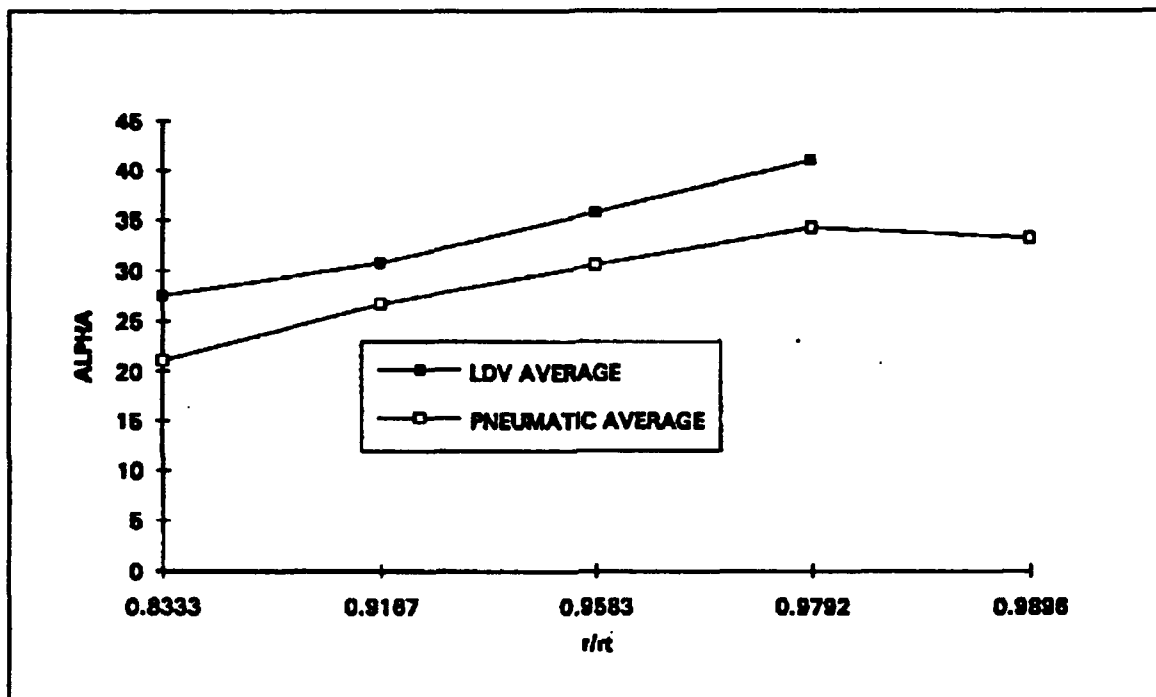
Figure 32.   Comparison of Stator LDV and Pneumatic Averages

60
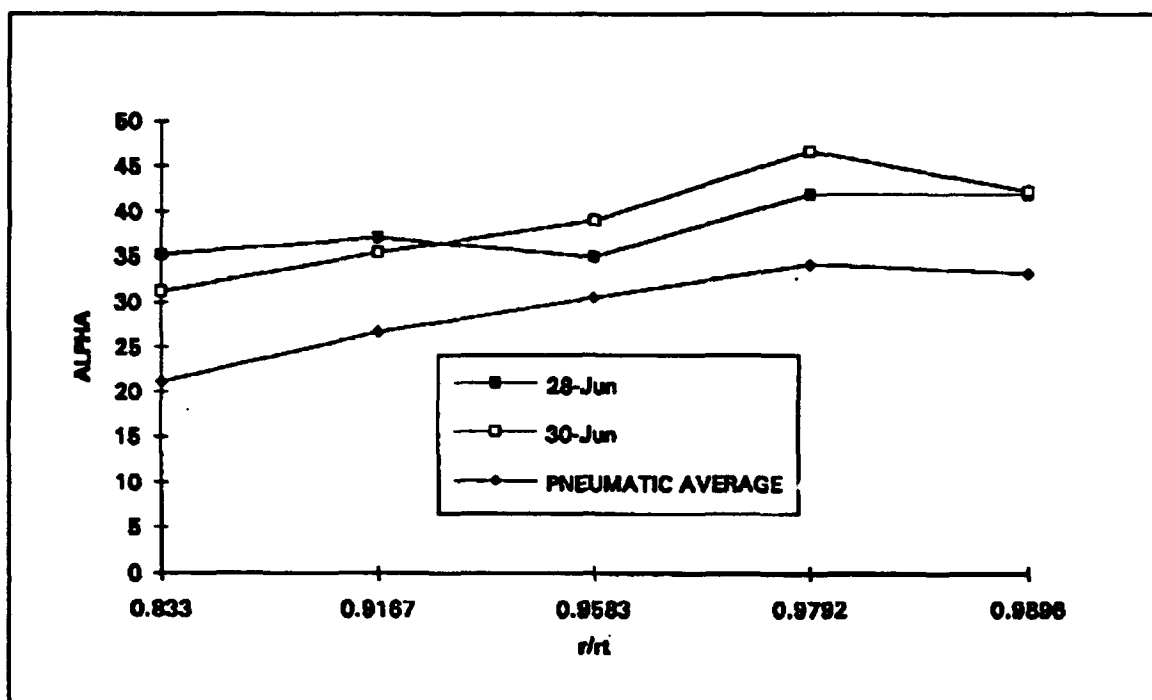
Figure 33.   Individual LDV Surveys vs. Pneumatic Average

V. CONCLUSIONS AND RECOMMENDATIONS

A. CONCLUSIONS

Two-component LDV measurements of velocity within the LSMSC, indexed to rotor position, were obtained for the first time. The following conclusions were drawn:

- Good agreement with pneumatic probe measurements was demonstrated.

- The mean flow velocity were measured to decrease in the case wall boundary layer.

- Relative to the rotor, a circumferential velocity peak was measured in the circumferential position where it was calculated to be.

- There was increased unsteadiness in the flow towards the case wall.

- An axial velocity deficit was measured circumferentially in the wake of the rotor.

- Good wake definition was found in the 1/8 inch upstream survey.

- LDV measurements downstream of the stator were in agreement with the pneumatic probe measurements.

- The rotor wake was no longer defined after passage through the stator.

B. RECOMMENDATIONS

Several recommendations are made concerning the LDV equipment. First, given the relatively slow rate of data acquisition experienced during the present experiment, the

acquisition of a TSI IFA 750 digital burst correlator is highly recommended for additional work on the LSMSC.

There is a large clear window on the LSMSC directly over the first rotor row on top of the compressor. The opening is suitable to conduct three-dimensional LDV measurements in the compressor. Means should be found to take advantage of this opportunity and the chance to validate Moyle's work on tip clearance effects [Ref 6]. In addition, the expanded measurement window would give a researcher much greater axial and circumferential freedom to explore the flow within the rotor itself.

Seeding must be introduced further upstream and in greater quantity to ensure a more even distribution throughout the rotor. With the approximately 60° swirl velocity present in the compressor, the introduction of the seed must be planned accordingly. Given that the compressor exhausts directly into the room, continued use of organic seed is recommended.

The TSI PHASE software should be modified to allow the collection of data points to be the limiting factor rather than the current limitation of a 1000 second DMA Timeout. Because of the relatively low data rate experienced, the time limitation on the data collection severely hindered turbulence and wake profile analysis.

Additionally, an entire suite of software programs must be written to fully analyze future PHASE data acquisition. Programs to analyze and graphically overlay results from

individual blade passages, non-dimensionalize the data, and analyze rotor-indexed data after passage through a stator passage, are examples of what is recommended. Given the size of an average PHASE data file, such programs are guaranteed to outstrip the storage, memory, and processing capability of personal computers. The acquisition of an advanced workstation or small mainframe is recommended.

APPENDIX I. COMPRESSOR PNEUMATIC INSTRUMENTATION

The compressor had two different classifications of instruments associated with the various data collection methods. The low response instrumentation measured predominantly the fairly constant pressures from pneumatic probes and static pressure taps. This was used for point-to-point surveys to determine overall performance and velocity triangle data. High response instrumentation, on the other hand, involved the collection of copious amounts of data from a semi-conductor transducer inserted at a limited number of fixed points. This did, however, allow a much greater spatial and temporal resolution in results versus low response instrumentation.

A. COMPRESSOR INSTRUMENTATION

1. Low Response Instrumentation

The instrumentation found on the compressor consisted of over 60 pneumatic probes as well as eleven other non-pressure devices. The pressure instrumentation included two United Sensor five hole probes and one three hole cobra probe for radial surveys between the stages, four Kiel Probes, a total pressure (Pitot) probe, a 12 port inlet pressure (radial) rake, a 12 port exit pressure (radial) rake and numerous static pressure taps. Non-pressure devices include

three battery-operated ice-point thermocouples, a magnetic tachometer, a torquemeter, and six linear potentiometers to record radial and yaw positions of the three movable probes. Figure A1 shows the position of each on the compressor.

Waddell, in his 1982 thesis [Ref. 9], describes the operation and location of the instrumentation in some detail. The changes made by Moyle and others, as well as the author, warrant a repeat of the description.

The pressure sensors were connected to one of the two Scanivalves used in this experiment. Prior to running, on-line scale verification was conducted. Port one of the Scanivalve was connected to the transducer reference pressure (atmo) to give the zero reading (or tare) for the transducer, while the second port was connected to a U-tube water manometer pressurized to a controlled air pressure (measured in inches of water). A second water manometer (vertical) was connected downstream of the first in order to help verify correct reference pressure settings. Moyle's technical note [Ref. 5] describes the operation of this second manometer in detail. Scale factor and zero drift were then checked at each data point. Once balanced, a reading other than zero at any port, besides port number two, automatically indicated a problem with that pressure sensor. The Scanivalve actuators were driven by the data acquisition controller and the pressures were measured by a 2.5 psig differential pressure transducer. Direct sunlight was found to interfere with the

66
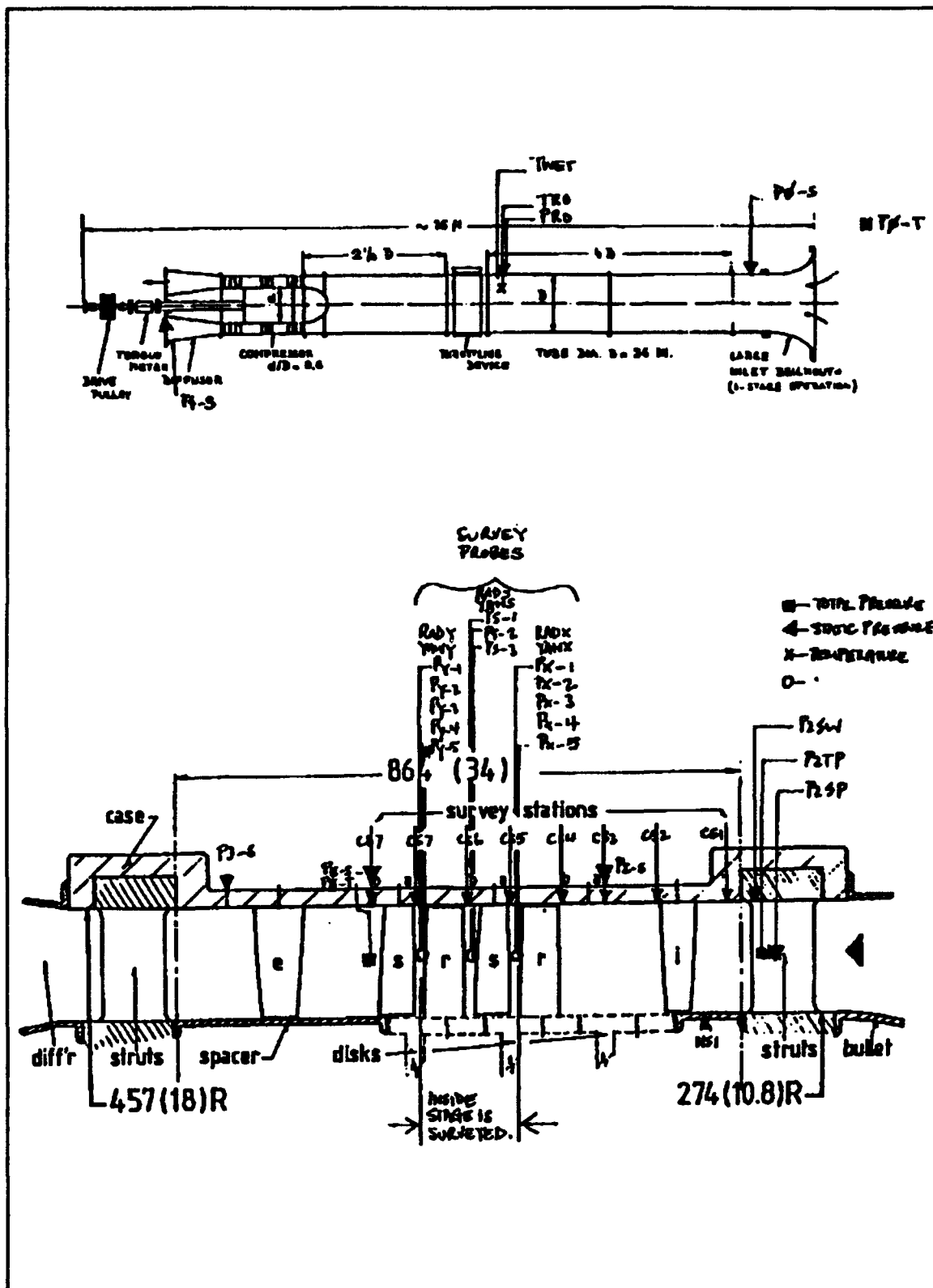
Figure A1.   Location and Types of Quantities Measured

balancing, therefore, the Scanivalve boxes were shielded from direct sunlight. For the purposes of the experiment, the zero offset was measured at the beginning (port number one) and at the end (port number 48) of each Scanivalve. Figure A2 shows the pneumatic measurement system schematic diagram. For pictorial clarity, the second manometer is not shown. Figure A3 shows a photograph of the equipment. The electrical signals from all the transducers were electronically conditioned before digitizing by the digital voltmeter.

Ambient pressure was measured in the building by an absolute pressure transducer connected to port number three on both Scanivalves, although previous experience dictated a manual entry of barometer readings due to excessive drift in the absolute transducer [Ref. 9]. Inlet total temperature was measured using two "J" type thermocouples at the inlet. Total temperature rise was measured by averaging the outputs of the two "J" thermocouple located at mid radius at the stator exit and comparing them with the measurements taken at the inlet. The parallel connections of all thermocouples into a dissimilar metal junction panel prior to a thermocouple [Ref. 5] was replaced by an individual ice point for each temperature sensor.

Rotational speed of the compressor was measured using a magnetic pickup connected to a digital counter. Torque was measured using a Lebow Model 1215-6K torquemeter. Inlet bell-mouth (nozzle) mass flow rate was measured by using the
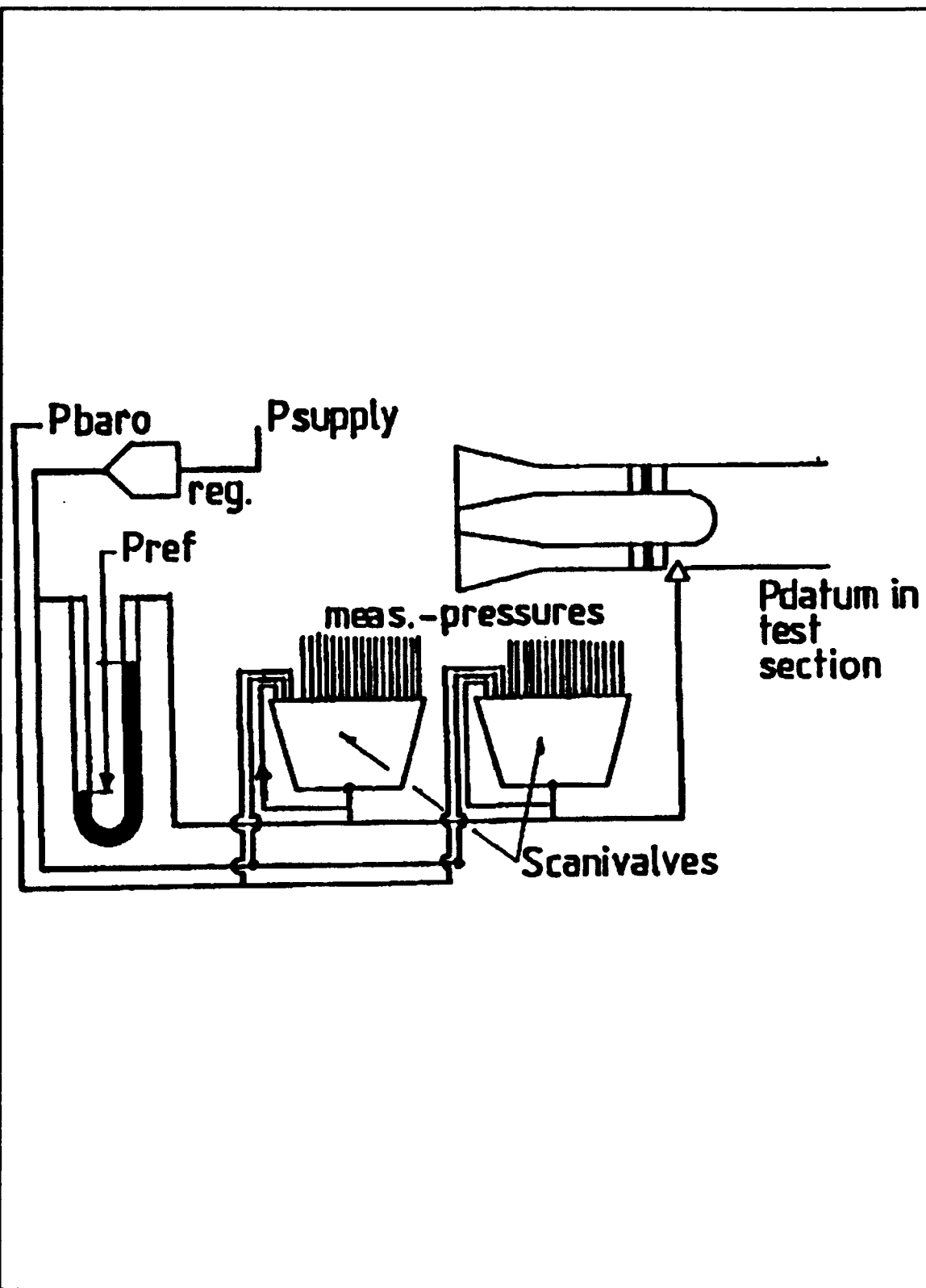
Figure A2. Pneumatic System Measurement Schematic
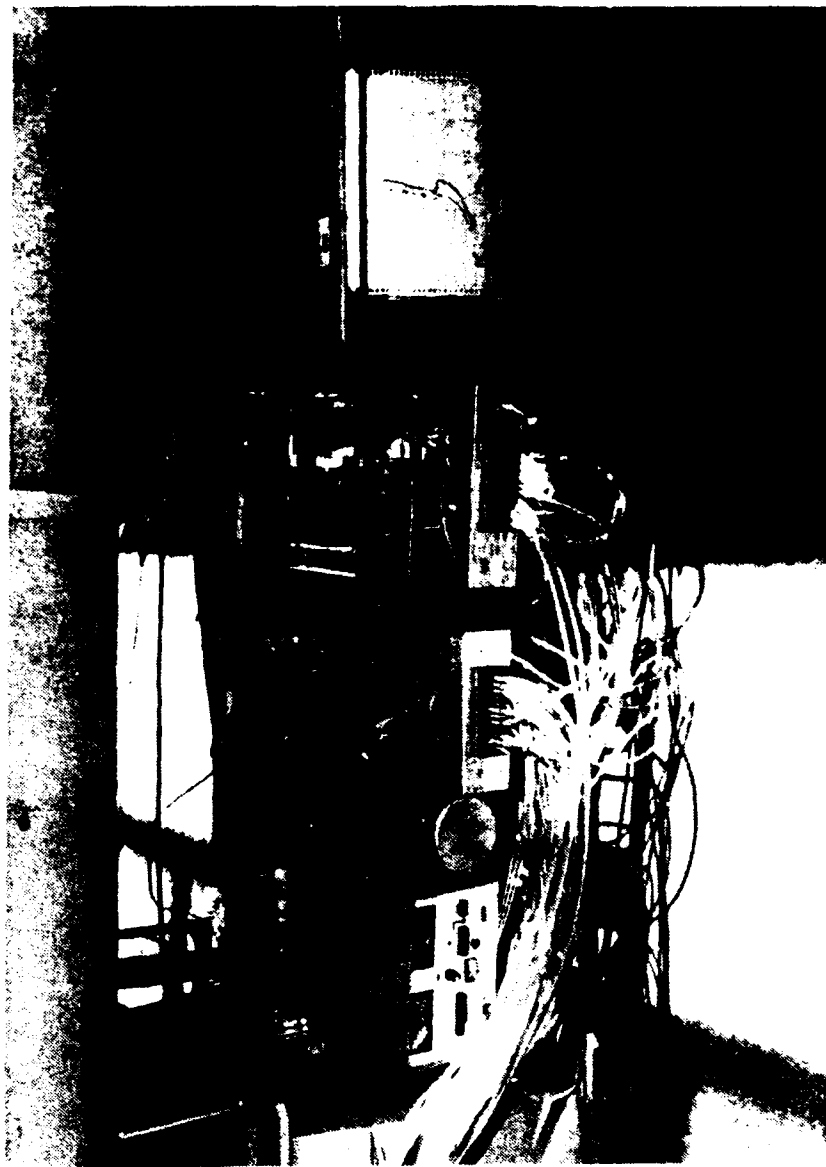
Figure A3.   Low Response System Measurement Equipment

differential between the (stagnation) pressure at the face of the inlet versus the (static) pressure in the throat. Port number one and 48 of both Scanivalves were connected to a total pressure tube two duct diameters downstream of the inlet screens (throttle). This reading was used only for verification and was not used for calculations.

Within the test section itself, mid-span total pressure was measured by the Pitot tube, while the total hub-to-tip pressure distribution was measured by the 12 hole inlet rake. Total pressure was determined by mass averaging [Ref. 9]. Exit total pressure was measured and calculated in the same fashion as the inlet rake. Eight case wall static pressure taps and two hub static pressure taps were used to monitor pressure rise through the compressor. The pressure rise was determined using averaged wall static taps upstream and downstream of the stages. Four Kiel probes at the stator exit completed the instrumentation on the first Scanivalve.

The second Scanivalve was used for the two five-hole (X and Y) probes as well as the cobra (S) probe. The planes of measurement are shown in Figure A4. The radial positions and yaw angles were recorded from the potentiometer attached to the probe mounts. The "X" probe and the "S" probe were adjusted by hand, while the "Y" probe was driven by electric motors. The probes were null-yawed by balancing a water manometer connected to each of the yaw ports. Accuracy in the yaw balancing was crucial, though difficult to obtain due to

71
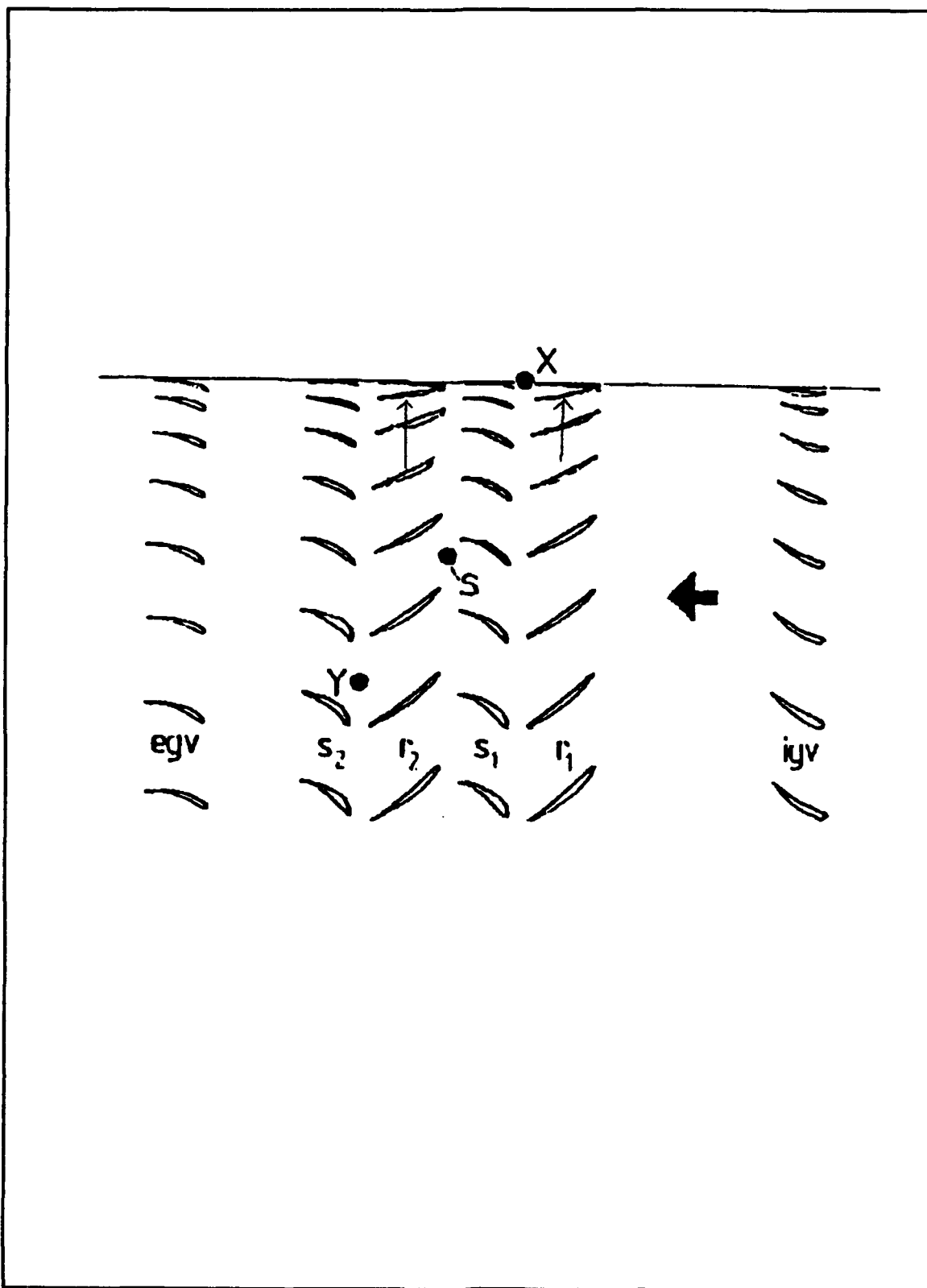
Figure A4. Radial Probe Locations Relative to Blading

the flow unsteadiness within the blade rows.

2. High Response Instrumentation

High response instrumentation consisted mainly of a Kulite pressure transducer described in detail in Reference 6. The Kulite probe could be positioned in any one of 30 holes drilled in a plate located over the second rotor row (six holes axially by five holes circumferentially). The position of the rotor was precisely phase-locked by means of a magnetic pickup, which in turn triggered a signal generator. A stroboscope was then triggered by the signal generator for visual verification of blade position; a Plexiglas window was located over the first rotor row for precisely this purpose. Should the rotor position have moved, it could be repositioned using the signal generator to adjust the timing of the stroboscope.

The signal passing from the Kulite probe entered a signal conditioning unit for zero-balancing and ranging prior to being sent to the Data Acquisition System. All three signals, the phase-locked signal, the Kulite probe signal, and the signal generator signal were all monitored by means of an oscilloscope. Figure A5 shows a photograph of this equipment.
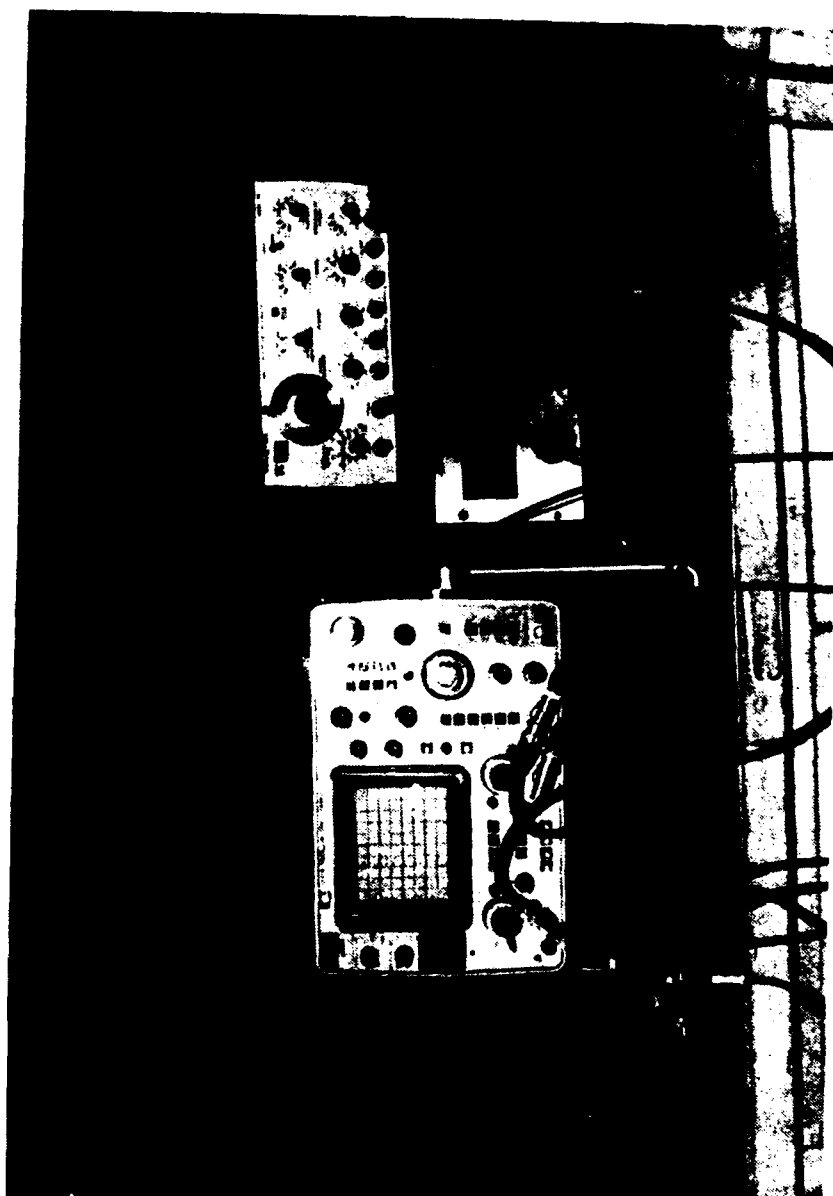
Figure A5.   High Response Measurement Equipment

B. PNEUMATIC DATA ACQUISITION SYSTEM

1. Low Response Data Acquisition Instrumentation

Data acquisition for this portion of the experiment was conducted using a Hewlett Packard 9000/300 controller and a HP 98032A interface bus. Acquisition components on the bus included a digital voltmeter, system voltmeter, scanner and Scanivalve control unit. Figure A6 shows the setup. The controller directed a sweep of the Scanivalve, with a reading of one port taking approximately one second. The controller directed three measurements of each port. Three passes were made over each Scanivalve. Both pneumatic and non-pneumatic data was processed through the digital voltmeter and ensemble averaged. Data were then stored to the data file specified. The software used is described in detail in Reference 10 [Ref. 10]. Tables AI and AII show the "look-up tables" for the data collected for each low response survey.

2. High Response Data Acquisition Instrumentation

The high response data acquisition instrumentation used much of the same equipment as the low response data acquisition system, with the exception of the high speed analog-to-digital system voltmeter. The system voltmeter was limited to 5000 readings per second.

Figure A6.   Compressor Pneumatic Control Equipment

76

TABLE AI.   COMPRESSOR PERFORMANCE DATA

		vblname	vno	vcralf	t	sc	chl	dely	rno	rdly	open	dyn	vrefvel
98	!	hkp_cc											
99	!	vblname vno vcralf t sc chl dely rno rdly open dyn vrefvel											
100	!	name scale no. channel											reference value
101	!	P8AR	1	1	0	0	0	0	0	0	•	•	30.0
102	!	Pabs	50	10000	0	1	20	•	10	•	•	•	30.0
103	!	FRLD	7	1	0	0	0	0	0	0	•	•	305.4
104	!	F8fv	11	10000	0	1	12	•	•	•	•	•	0.0
105	!	TRQ	8	10000	0	1	9	•	10	•	•	•	0.0
106	!	TWET	3	10000	3	1	13	•	•	•	•	•	0.0
108	!	TAMB	2	1000	1	1	5	0	5	0	•	•	0.0
109	!	OT-1	9	10000	2	1	6	•	•	•	•	•	0.0
110	!	OT-2	10	10000	2	1	7	•	•	•	•	•	0.0
111	!	TORQ	6	10000	0	1	30	•	20	•	•	•	0.0
112	!	P021	191	10000	0	2	1	•	•	•	•	•	0.0
113	!	P12	190	10000	0	2	2	•	•	•	•	•	0.0
114	!	P•2	196	10000	0	2	3	•	•	•	•	•	0.0
115	!	P0-T	12	10000	0	2	4	•	•	•	•	•	0.0
116	!	P0-S	13	10000	0	2	5	•	•	•	•	•	0.0
117	!	PRO	93	10000	0	2	6	•	•	•	•	•	0.0
118	!	P2SW	84	10000	0	2	7	•	•	•	•	•	0.0
119	!	P21P	85	10000	0	2	8	•	•	•	•	•	0.0
120	!	P2SP	86	10000	0	2	9	•	•	•	•	•	0.0
121	!	PE-T	87	10000	0	2	10	•	•	•	•	•	0.0
122	!	PI-S	88	10000	0	2	11	•	•	•	•	•	0.0
123	!	PE-S	89	10000	0	2	12	•	•	•	•	•	0.0
124	!	PP-1	70	10000	0	2	13	•	•	•	•	•	0.0
125	!	PP-2	71	10000	0	2	14	•	•	•	•	•	0.0
126	!	PP-3	72	10000	0	2	15	•	•	•	•	•	0.0
127	!	PP-4	73	10000	0	2	16	•	•	•	•	•	0.0
128	!	PP-5	74	10000	0	2	17	•	•	•	•	•	0.0
129	!	PP-6	75	10000	0	2	18	•	•	•	•	•	0.0
130	!	PP-7	76	10000	0	2	19	•	•	•	•	•	0.0
131	!	PP-8	77	10000	0	2	20	•	•	•	•	•	0.0
132	!	PP-9	78	10000	0	2	21	•	•	•	•	•	0.0
133	!	PP-0	79	10000	0	2	22	•	•	•	•	•	0.0
134	!	PP-A	80	10000	0	2	23	•	•	•	•	•	0.0
135	!	PP-B	81	10000	0	2	24	•	•	•	•	•	0.0
136	!	HS1	29	10000	0	2	37	•	•	•	•	•	0.0
137	!	CS1	20	10000	0	2	38	•	•	•	•	•	0.0
138	!	CS2	21	10000	0	2	39	•	•	•	•	•	0.0
139	!	CS3	22	10000	0	2	40	•	•	•	•	•	0.0
140	!	CS4	23	10000	0	2	41	•	•	•	•	•	0.0
141	!	CS5	24	10000	0	2	42	•	•	•	•	•	0.0
142	!	CS6	25	10000	0	2	43	•	•	•	•	•	0.0
143	!	CS7	26	10000	0	2	44	•	•	•	•	•	0.0
144	!	CS8	27	10000	0	2	45	•	•	•	•	•	0.0
145	!	P3-S	31	10000	0	2	46	•	•	•	•	•	0.0
146	!	P4-S	32	10000	0	2	47	•	•	•	•	•	0.0
147	!	P022	192	10000	0	2	48	•	•	•	•	•	0.0
148	!	TBRGF	199	10000	0	1	8	•	•	•	•	•	0.0

✦ = a default value defined in program

77

TABLE AII. COMPRESSOR RADIAL SURVEY DATA

		hkp_vd											
98		vblname	vno	vscalf	t	sc	chl	dely	rno	rdly	open	dyn	vrefval
99		....	...	......	.	..	...	....	...	....	....	...	....
100													
101		PBAH	1		1	0	0	0	0	0	0	•	•	30.0
102		Pabs	1	10000	1	1	20	•	10	•	•	•	30.0
103		FULO	7		1	0	0	0	0	0	•	•	805.4
106		FNFv	11	10000	0	1	12	•	•	•	•	•	805.4
107		TRO	8	10000	0	1	9	•	10	•	•	•	0.0
108		TNET	3	10000	0	1	13	•	•	•	•	•	0.0
109		P021	191	10000	0	2	1	•	•	•	•	•	0.0
110		Ps2	190	10000	0	2	2	•	•	•	•	•	0.0
111		P-2	198	10000	0	2	3	•	•	•	•	•	0.0
112		PO-1	12	10000	0	2	4	•	•	•	•	•	0.0
113		PO-3	13	10000	0	2	5	•	•	•	•	•	0.0
114		PRO	93	10000	0	2	6	•	•	•	•	•	0.0
115		P25W	84	10000	0	2	7	•	•	•	•	•	0.0
116		P21P	85	10000	0	2	8	•	•	•	•	•	0.0
117		P25P	86	10000	0	2	9	•	•	•	•	•	0.0
118		PE-1	87	10000	0	2	10	•	•	•	•	•	0.0
119		PI-3	88	10000	0	2	11	•	•	•	•	•	0.0
120		PE-5	89	10000	0	2	12	•	•	•	•	•	0.0
121		HSI	28	10000	0	2	37	•	•	•	•	•	0.0
122		CS1	20	10000	0	2	38	•	•	•	•	•	0.0
123		CS2	21	10000	0	2	39	•	•	•	•	•	0.0
124		CS3	22	10000	0	2	40	•	•	•	•	•	0.0
125		CS4	23	10000	0	2	41	•	•	•	•	•	0.0
126		CS5	24	10000	0	2	42	•	•	•	•	•	0.0
127		CS5	25	10000	0	2	43	•	•	•	•	•	0.0
128		CS7	26	10000	0	2	44	•	•	•	•	•	0.0
129		CS0	27	10000	0	2	45	•	•	•	•	•	0.0
130		P3-S	31	10000	0	2	46	•	•	•	•	•	0.0
131		P4-S	32	10000	0	2	47	•	•	•	•	•	0.0
132		P022	192	10000	0	2	48	•	•	•	•	•	0.0
133		P031	194	10000	0	3	1	•	•	•	•	•	0.0
134		Ps3	193	10000	0	3	2	•	•	•	•	•	0.0
135		P-3	197	10000	0	3	3	•	•	•	•	•	0.0
136		TAMB	2	1000	1	1	5	•	10	•	•	•	0.0
137		PX-1	33	10000	0	3	15	•	•	•	•	•	0.0
138		PX-2	34	10000	0	3	16	•	•	•	•	•	0.0
139		PX-3	113	10000	0	3	17	•	•	•	•	•	0.0
140		PX-4	35	10000	0	3	18	•	•	•	•	•	0.0
141		PX-5	36	10000	0	3	19	•	•	•	•	•	0.0
142		PY-1	37	10000	0	3	20	•	•	•	•	•	0.0
143		PY-2	38	10000	0	3	21	•	•	•	•	•	0.0
144		PY-3	114	10000	0	3	22	•	•	•	•	•	0.0
145		PY-4	39	10000	0	3	23	•	•	•	•	•	0.0
146		PY-5	40	10000	0	3	24	•	•	•	•	•	0.0
147		PS-1	45	10000	0	3	30	•	•	•	•	•	0.0
148		PS-2	116	10000	0	3	31	•	•	•	•	•	0.0
149		PS-3	117	10000	0	3	32	•	•	•	•	•	0.0
150		P032	195	10000	0	3	48	•	•	•	•	•	0.0
151		RAUX	66	1000	0	1	31	•	•	•	•	•	0.0
152		YAWX	62	10000	0	1	32	•	•	•	•	•	0.0
153		RAUY	58	10	0	1	33	•	•	•	•	•	0.0
154		YAWY	57	1000	0	1	34	•	•	•	•	•	0.0
155		RADS	53	10	0	1	35	•	•	•	•	•	0.0
156		YAWS	54	1000	0	1	36	•	•	•	•	•	0.0
157		IBR6F	199	10000	0	1	0	•	•	•	•	•	0.0

APPENDIX II. DATA REDUCTION PROGRAMS

The following are two programs used in reducing the LDV data for comparison with pneumatic probe data. The programs involve simple averaging of columns of numbers. Although there were many commercially available spreadsheets that could easily perform the same function, they were limited in the number of lines of data that they could process.

The PHASE raw data were initially converted to ASCII data by means of a TSI proprietary program called PHASRTOA. After conversion, the following programs were applied to each data file. Most files contained data taken in the coincidence mode and as a result, the first program was used.

The general logic of the programs is as follows: first, the data file is read into the program. The Doppler frequency is found by multiplying the number of fringes in the probe volume by the time the particle is inside the probe volume. It is then multiplied by the fringe spacing to obtain the velocity. For the U velocity the equation is as follows:

$$vel_1 = (4.7523E^-6) \, n_{fr} / (time_1) \, 1E^-9 \qquad (1)$$

The V velocity equation is as follows:

$$vel_2 = (4.51119E\text{-}6)\, n_{fr} / (time_2)\, 1E\text{-}9 \qquad (2)$$

The LDV angle is given by the following equation:

$$\alpha = 90 - \arctan(V/U) \qquad (3)$$

```fortran
      program average
c------------------------------------------------------------
This program reads the output from PHASE collected in the
coincidence mode and averages all the velocities
calculated from the raw data ASCII file.
c------------------------------------------------------------
      character*10 fame
        print *,'Input the raw ASCII file name:-'
        read *,fame
        print *,fame
        open(unit=10,file=fame,status='unknown')
c
        m=0
        sum2=0.
        sum1=0.
c
c     Prompt for no. of data points
c
        print *,'Input the number of data points:-'
        read *,nn
c
        do 10 i=1,nn
        m=m+1
        read(10,100)n,nch2,nfr2,time2,nch1,nfr1,time1,nencod
  100   format(i9,i3,i4,e13.6,i2,i4,e13.6,i6)
        freq2=nfr2/(time2*1.e-09)
        freq1=nfr1/(time1*1.e-09)
        vel2=(4.5119*1.e-06)*freq2
        vel1=(4.7523*1.e-06)*freq1
        print *,n,vel2,vel1
        sum2=sum2+vel2
        sum1=sum1+vel1
   10   continue
c
c     Compute the average
c
        av2=sum2/m
        av1=sum1/m
        print *,' Average velocity U (for channel 1) is ',av1
        print *,
        print *,' Average velocity V (for channel 2) is ',av2
        end
```

```
      program ravg (random average)
c------------------------------------------------------------
This program reads the output from PHASE collected in the
random mode and averages all the velocities calculated from
 the raw data ASCII file.
c------------------------------------------------------------
      character*10 fame
      print *,'Input the raw ASCII file name:-'
      read *,fame
      print *,fame
      open(unit=10,file=fame,status='unknown')
c
      nch1=0
      nch2=0
      sum2=0.
      sum1=0.
c
c     Prompt for no. of data points
c
      print *,'Input the number of data points:-'
      read *,nn
c
      do 10 i=1,nn
      read(10,100)n,nch,nfr,time,nencod
  100 format(i9,i3,i4,e13.6,i6)
      freq=nfr/(time*1.e-09)
      if (nch .eq. 2) then
      nch2=nch2+1
      vel2=(4.5119*1.e-06)*freq
      print *,n,vel2
      sum2=sum2+vel2
      end if
      if (nch .eq. 1) then
      nch1=nch1+1
      vel1=(4.7523*1.e-06)*freq
      print *,n,vel1
      sum1=sum1+vel1
      end if
   10 continue
c
c     Compute the average
c
      av2=sum2/nch2
      av1=sum1/nch1
      print *,' Average velocity U (for channel 1) is ',av1
      print *,
      print *,' Average velocity V (for channel 2) is ',av2
      end
```

APPENDIX III. TEST REFERENCE DATA

The following is a table of pneumatic quantities taken for non-dimensionalization purposes.

TABLE AIII. PNEUMATIC QUANTITIES MEASURED

	28 JUN				02 JUL		
r/r_t	P_0	T_0	Pitot		P_0	T_0	Pitot
ROTOR							
0.8889	.15"	68°F	6.7"		.15"	64°F	6.5"
0.9167	.15"	68°F	6.7"		.15"	66°F	6.5"
0.9444	.15"	68°F	6.7"		.15"	66°F	6.5"
0.9722	.15"	67°F	6.7"		.15"	68°F	6.5"
0.9862	.15"	----	6.7"		.15"	68°F	6.5"
STATOR							
0.8333	.15"	68°F	6.5"		.15"	68°F	6.5"
0.9167	.15"	68°F	6.5"		.15"	68°F	6.5"
0.9583	.15"	68°F	6.5"		.15"	68°F	6.5"
0.9792	.15"	68°F	6.5"		.15"	68°F	6.5"
0.9896	.15"	68°F	6.5"		.15"	68°F	6.5"

LIST OF REFERENCES

1. Strazisar, A.J., "Application of Laser Anemometry to Turbomachinery Flowfield Measurements", Lecture Notes for Lecture Series No. 3 at the von Karman Institute for Fluid Dynamics, Rhode-Saint_genese, Belgium, 1985.

2. Stauter, R.C., Dring, R.P., and Carta P.O., "Temporally and Spatially Resolved Flow in a Two-Stage Axial Compressor: Part I - Experiment," ASME Journal Of Turbomachinerey, v. 113, No 2, pp. 219-226.

3. Stauter, R.C., "Measurement of the Three-Dimensional Tip Region Flowfield in an Axial Compressor," ASME paper 92-GT-211, 1992.

4. Chesnakas, C.J. and Dancey, C.L., "Three-Component LDA Measurements in an Axial-Flow Compressor," AIAA Journal of Propulsion and Power, v. 6, pp. 474-481, August 1990.

5. Moyle, I.N., "Multistage Compressor - Operation and Maintenance of the Low Speed Multistage Compressor Facility," Naval Postgraduate School, Monterey, California, Turbopropulsion Lab. TN/90-03, June, 1990.

6. Moyle, I.N., "An Experimental and Analytic Study of Tip Clearance Effects In Axial Flow Compressors," Doctoral Dissertation, University Of Tasmania, Australia, December 1991; also Contractor Report NPS AA-92-001CR, Naval Postgraduate School, Monterey California, December 1991.

7. Moyle, I.N., "Multistage Compressor - Advanced Aerodynamic Flow Field Experiments," Naval Postgraduate School, Monterey, California, Turbopropulsion Lab. TN/90-01, June, 1990.

8. Vavra, M.H., "Aerodynamic Design of Symmetrical Blading for a Three-Stage Axial Flow Compressor Test Rig," Naval Postgraduate School, Monterey, California, NPS-57-Va73121A, 1973.

9. Waddell, J.L., "Evaluation of the Performance and Flow in an Axial Compressor," Master's Thesis, Naval Postgraduate School, Monterey, California, March, 1983.

10. Moyle, I.N., "Multistage Compressor - Data Acquisition System and Reduction Software (HP-9000/300)," Naval Postgraduate School, Monterey, California, Turbopropulsion Lab. TN/90-02, June, 1990.

INITIAL DISTRIBUTION LIST

		No. Copies
1.	Defense Technical Information Center Cameron Station Alexandria VA 22304-6145	2
2.	Library, Code 052 Naval Postgraduate School Monterey CA 93943-5002	2
3.	Department Chairman, AA Department of Aeronautics Naval Postgraduate School Monterey, California 93943	1
4.	Chairman, SSAG Space System Academic Group Naval Postgraduate School Monterey, California 93943	1
5.	Garth V. Hobson, Turbopropulsion Laboratory Code AA/Hg Department of Aeronautics Naval Postgraduate School Monterey, California 93943	6
6.	Director Navy Space Systems Division (N63) Space and Electronic Warfare Directorate Chief of Naval Operations Washington, DC 20350-2000	1
7.	Naval Air Warfare Center Aircraft Division (Trenton) PE-31 (Attn: S. Clouser) 250 Phillips Blvd Princeton Crossroads Trenton, New Jersey 08628-0176	1
8.	Joseph M. Utschig 10 Marion Ave Salinas, CA 93901	1